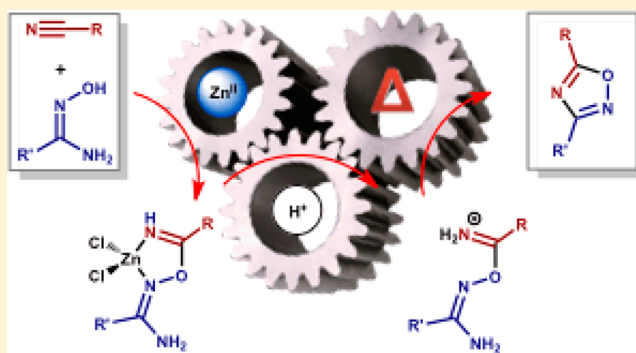


Zinc(II)-Mediated Nitrile–Amidoxime Coupling Gives New Insights into H⁺-Assisted Generation of 1,2,4-OxadiazolesDmitrii S. Bolotin,[†] Kirill I. Kulish,[†] Nadezhda A. Bokach,^{*,†} Galina L. Starova,[†] Vladislav V. Gurzhiy,[‡] and Vadim Yu. Kukushkin^{*,†,§}[†]Institute of Chemistry, Saint Petersburg State University, Universitetsky Pr. 26, 198504 Stary Petergof, Russian Federation[‡]Institute of Earth Sciences, Saint Petersburg State University, University emb. 7/9, 199034 Saint Petersburg, Russian Federation[§]Institute of Macromolecular Compounds of Russian Academy of Sciences, V.O. Bolshoi Pr. 31, 199004 Saint Petersburg, Russian Federation

Supporting Information

ABSTRACT: The cyanamides Me₂NCN (**1a**), OC₄H₈NCN (**1b**), and PhC(=O)N(H)CN (**1c**) and the conventional nitriles PhCN (**1d**) and EtCN (**1e**) react with 1 equiv of each of the amidoximes R'C(=NOH)NH₂ (R' = Me (**2a**), Ph (**2b**)) in the presence of 1 equiv of ZnCl₂ producing the complexes [ZnCl₂{HN=C(R)ON=C(R')NH₂}] (R/R' = NMe₂/Me (**3a**), NMe₂/Ph (**3b**), NC₄H₈O/Me (**3c**), NC₄H₈O/Ph (**3d**), N(H)C(=O)Ph/Me (**3e**), N(H)C(=O)Ph/Ph (**3f**), Ph/Me (**3g**), Ph/Ph (**3h**), Et/Ph (**3j**)) with the chelate ligands originating from the previously unreported zinc(II)-mediated nitrile–amidoxime coupling. Addition of 1 equiv of *p*-TolSO₃H to any of one **3a–h**, **3j** results in the ligand liberation and formation of the iminium salts [H₂N=C(R)ON=C(R')NH₂](*p*-TolSO₃) [**4a–j**](*p*-TolSO₃), which then at 20–65 °C spontaneously transform to 1,2,4-oxadiazoles (**5a–j**). As a side reaction, cyanamide derived species [**4a–f**](*p*-TolSO₃) undergo Tiemann rearrangement to produce the substituted ureas R'NHC(=O)NH₂ (R' = Me (**6a**), Ph (**6b**)) and RC(=O)NH₂ (R = NMe₂ (**6c**), NC₄H₈O (**6d**), N(H)C(=O)Ph (**6e**)), whereas phenyl and ethyl cyanide derivatives besides their transformation to the oxadiazoles undergo hydrolysis to the parent amidoxime R'C(=NOH)NH₂ (R' = Me (**2a**), Ph (**2b**)) and the carboxamides RC(=O)NH₂ (R = Ph (**6f**), Et (**6g**)). All new obtained compounds were characterized by HRESI-MS, IR, ATR-FTIR, ¹H NMR, CP-MAS TOSS ¹³C NMR, elemental analyses (C, H, N), and single crystal X-ray diffraction for seven species (**3a–e**, [**4b**](*p*-TolSO₃), and [**4d**](*p*-TolSO₃)). Two previously unknown heterocycles **5c** and **5e** were isolated and characterized by elemental analyses (C, H, N), HRESI-MS, IR, ¹H and ¹³C{¹H} NMR. The observed conversion of [**4a–j**](*p*-TolSO₃) to the 1,2,4-oxadiazoles uncovers the mechanism of the previously reported H⁺-assisted generation of these heterocycles (Augustine; et al. *J. Org. Chem.* **2009**, *74*, 5640).



INTRODUCTION

1,2,4-Oxadiazoles represent an important class of five-membered heterocycles, and their versatile chemistry has been repeatedly reviewed over the years.¹ The increased rate of publication on the oxadiazoles relates to the importance of these heterocycles and their derivatives in both material chemistry (e.g., they serve as components of polymers,^{1a} liquid crystals^{1a} and ionic liquids,^{1a,2} luminescent,^{1a,2b} optoelectronic materials,^{1a} and corrosion inhibitors³) and medicinal chemistry^{1a,4} (where the oxadiazoles are applied as antidiabetic,^{1a} anti-inflammatory,^{1a,5} antithrombotic,^{5b} antimicrobial,^{1a,2a,6} antitumor agents,^{1a,4,7} immunosuppressors^{1a,2a} and neuroprotective agents,^{1a,2a,4,8} and are compounds exhibiting fungicidal and larvicidal properties⁹).

Among the known synthetic strategies for generation of 1,2,4-oxadiazoles, the two most common approaches utilize nitrile oxides or amidoximes as starting materials.^{1a} The first

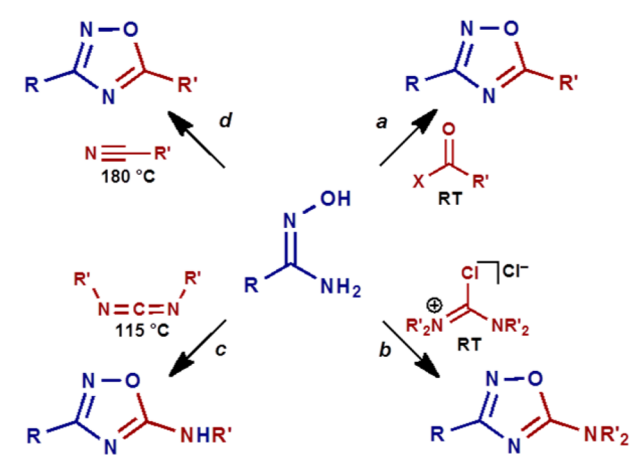
route includes 1,3-dipolar cycloaddition of nitrile oxides to nitriles^{2a} or 4-aryl-2-(alkylthio)-1-azetines.¹⁰ The second route (Scheme 1) is based upon reaction of amidoximes with activated derivatives of carboxylic acid (e.g., chloroanhydrides, anhydrides, or esters; (a)),^{1a} Vilsmeier salts¹¹ (b), carbodiimides^{5a} (c), or nitriles¹² (d).

Conditions of these reactions become more drastic on going from a to d. The syntheses of 1,2,4-oxadiazoles that are based on the reaction between the most unreactive R'CN substrates and amidoximes species require harsh conditions (180 °C, 24 h) when performed via metal-free protocols.¹³ However, these reactions could be conducted under substantially milder conditions (80 °C) in the presence of ZnCl₂ followed by addition of a strong acid (hereinafter the Zn^{II}/H⁺ system).^{12b–d}

Received: June 10, 2014

Published: September 8, 2014

Scheme 1. Amidoxime-Based Methods for Synthesis of 1,2,4-Oxadiazoles



Taking into account the great variety of commercially available nitriles, the application of the Zn^{II}/H^+ system places approach *d* among the most advantageous methods for preparation of 1,2,4-oxadiazoles.

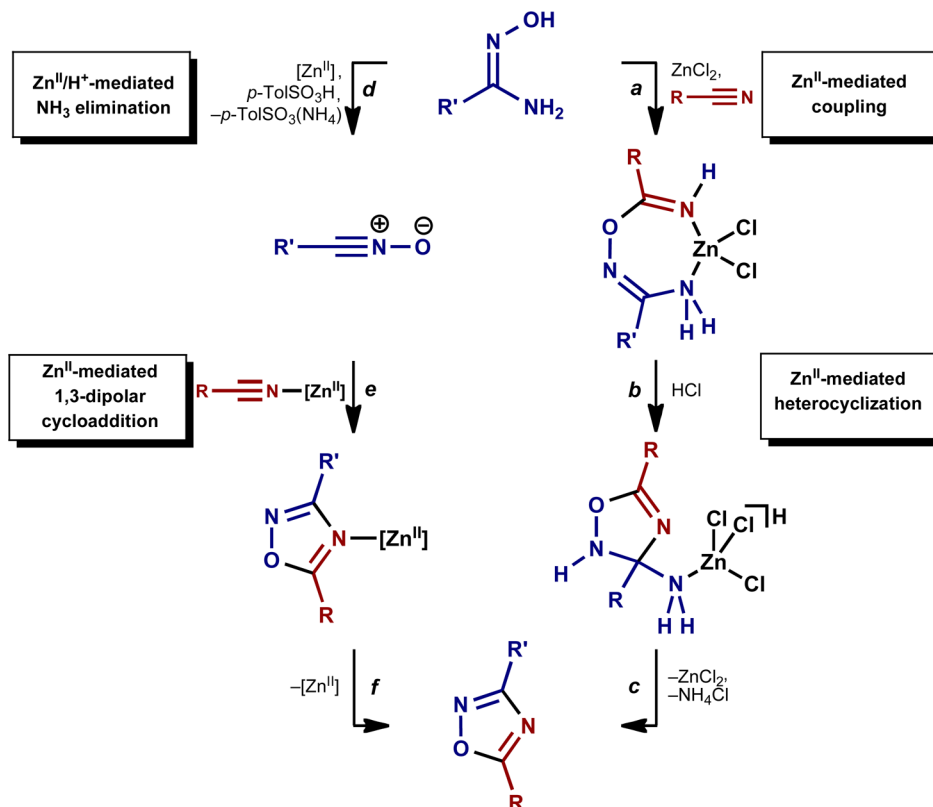
The Zn^{II}/H^+ -assisted reaction leads to 3,5-disubstituted 1,2,4-oxadiazoles, and two alternative mechanisms for this process were suggested. Yarovenko et al. on the basis of ^{15}N NMR data proposed that the reaction proceeds via nucleophilic addition of amidoximes to nitriles (Scheme 2, *a*) followed by metal-mediated heterocyclization of the ligand (*b*) promoted by a protonation with HCl.^{12c} In the subsequent work,^{12b} Augustine et al. suggest that the first step of the reaction includes formation of the nitrile oxide $R'CNO$ and elimination

of ammonia from the amidoxime by its treatment with the strong acid (*p*-TolSO₃H) (*d*), followed by 1,3-dipolar cycloaddition of thus generated $R'CNO$ to a coordinated nitrile (*e*). In all these works^{12b,c} describing the Zn^{II}/H^+ -assisted synthesis of 1,2,4-oxadiazoles, structures of the intermediates of the reaction were postulated, but not confirmed experimentally.

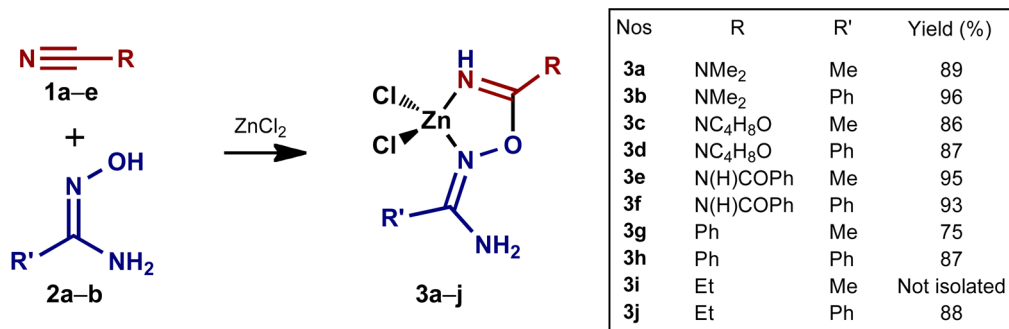
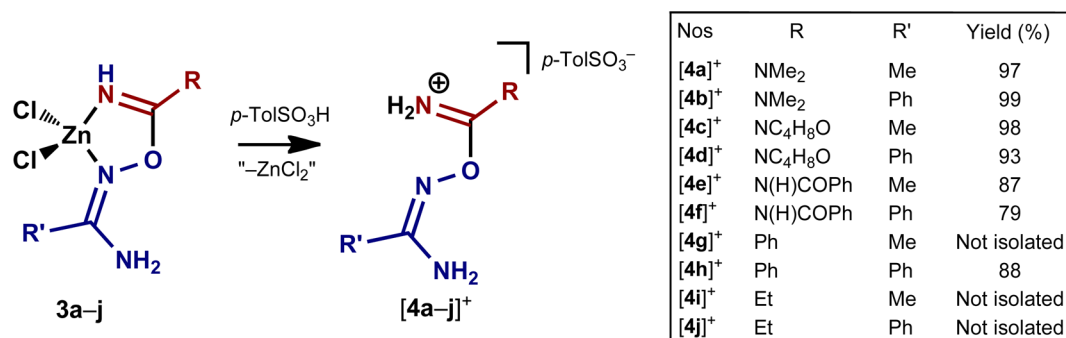
In view of our general interest to reactions of metal-activated nitriles (for our reviews see ref 14; for other reviews on this topic see refs 14d and 15) and also to coordination chemistry of amidoximes (for our reviews see refs 14b and 16 and for recent works see refs 12a and 17), we felt that the *organic chemistry* approach—that is directed toward final organic products with a rather little attention to metal-involving activation system—could be efficiently combined with the *inorganic chemistry* approach that includes the detection and identification of acting metal species. If the former approach is useful from a synthetic viewpoint, the latter is efficient for understating mechanisms and driving forces of studied synthetic transformations. Thus, we decided to verify the role of the Zn^{II} center in the synthesis of the oxadiazoles^{12b} by generation, isolation, and identification of zinc species formed upon nitrile–amidoxime reaction, and our results are reported in sections that follow.

RESULTS AND DISCUSSION

Zn^{II} -Mediated Nitrile–Amidoxime Coupling. As the starting materials for this study we addressed, on the one hand, the cyanamides Me_2NCN (**1a**), OC_4H_8NCN (**1b**), and $PhC(=O)N(H)CN$ (**1c**), as well as conventional nitriles, viz. benzonitrile $PhCN$ (**1d**) and propanenitrile $EtCN$ (**1e**). On the other hand, the amidoximes $R'C(=NOH)NH_2$ ($R' = Me$ (**2a**), Ph (**2b**)) were taken as the reaction partners. Cyanamides **1a–c** and nitriles **1d,e** react with 1 equiv of amidoximes **2a,b** in all

Scheme 2. Two Postulated Mechanisms of Zn^{II}/H^+ -Assisted Generation of 1,2,4-Oxadiazoles

Scheme 3. Generation of 3a–j via the Zinc(II)-Mediated Coupling

Scheme 4. Generation of [4a–j](*p*-TolSO₃) from 3a–j by the Acid Treatment

possible combinations in the presence of 1 equiv of ZnCl₂ (ethyl acetate, 20–48 h, 80 °C) producing zinc(II) chelates 3a–j that, apart from 3i, were isolated in 75–96% yields (Scheme 3). Complex 3i rapidly decomposes under the reaction conditions and it was not isolated from the reaction mixture. However, its generation was confirmed by HRESI⁺-MS (found, *m/z* 227.9879 [3i – Cl]⁺; calcd, 227.9877).

The observed coupling at the zinc(II) center was not previously reported, it is selective and no other zinc complexes were detected even if the starting organic reactants were taken in 4-fold excess with respect to ZnCl₂ (3a–h), or if the reaction with 1 equiv of 2a,b and 1 equiv of ZnCl₂ proceeds in the appropriate neat nitrile (3i,j).

No reaction was observed between 1a–e and 2a,b (in all combinations) in ethyl acetate for 2 days at temperatures ranging from 20 to 80 °C either in the presence of 1 equiv of *p*-TolSO₃H or without the acid. Attempted reaction was monitored by ESI-MS and ¹H NMR spectroscopies by analyzing residues formed after evaporation of EtOAc and their redissolution in (CD₃)₂SO. All these blank experiments point out that the observed nitrile–amidoxime coupling is zinc(II)-mediated.

As can be inferred from the synthetic experiment, the reactivity decreases in the following order R₂NCN ≥ ArCN > AlkCN that is in good agreement with the previously reported cyanide reactivity.^{17b,18} Thus, formation of 3a–f proceeds even with 1 equiv of the cyanamide for 20 h at 80 °C, whereas generation of 3g,h requires 4-fold excess of the nitrile and heating for 2 days. The most unreactive aliphatic nitrile, EtCN, forms 3i,j only under heating of the amidoximes in the neat nitrile at 65 °C for 2 days.

Metal-mediated iminoacylation of oximes is the rapidly developing field for the past two decades.^{14b} This reaction was observed at both kinetically inert (Pt^{IV},^{12a,19} Pt^{II},^{17,20} Re^{IV},²¹

Rh^{III,22}) and more labile (V^V,²³ Pd^{II},²⁴ Ni^{II,25}) metal centers. The iminoacylation that is mediated by the inert centers proceeds via *intermolecular* nucleophilic addition of an oxime to a nitrile ligand, whereas the reaction at the labile centers typically occurs via ligation of an oxime to a metal followed by *intramolecular* nucleophilic attack of the oxime HO group to the C≡N moiety. Noteworthy that metal-mediated reactions between ketoximes and nitriles also occurs at Co^{II}²⁶ and Zn^{II}^{12b–d,27} metal centers, but they lead to amidines,²⁶ carboxamides,²⁷ and 1,2,4-oxadiazoles,^{12b–d} and no iminoacylated oximes were detected. However, the latter species were postulated as plausible reaction intermediates.^{12c,25a,27}

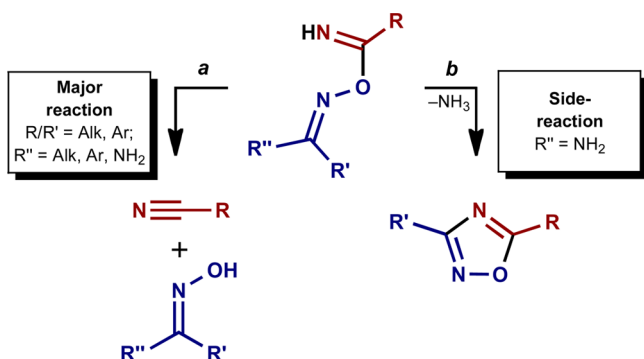
Liberation of the Chelated Ligands from Their Complexes. When a solution of 1 equiv of *p*-TolSO₃H in MeOH was added to a vigorously stirred suspension of any of one 3a–h or 3j in methanol, instantaneous homogenization of reaction mixtures was observed. Thus, formed solution contains organic salt [4a–h](*p*-TolSO₃) or [4j](*p*-TolSO₃) (Scheme 4), respectively, along with some zinc(II) species (e.g., [ZnCl₃][–] that was detected by ESI-MS). After the solvent was evaporated to dryness, [4a–d](*p*-TolSO₃), [4f](*p*-TolSO₃), and [4h](*p*-TolSO₃) were separated from zinc(II)-containing products by washing with ethyl acetate that dissolves all Zn^{II} species, whereas the organic salts are poorly soluble in EtOAc and they were separated by filtration. As an exception, [4e](*p*-TolSO₃) exhibits substantial solubility in all solvents where zinc species are also soluble (MeOH, EtOH, THF, EtOAc, and 1,4-dioxane) and, therefore, [4e](*p*-TolSO₃) cannot be purified by the described method. This compound was isolated in a pure form by precipitation of the known (NMe₄)₂[ZnCl₄]²⁸ from the reaction mixture by the treatment with 2 equivs of (NMe₄)Cl. Pure [4a–f](*p*-TolSO₃) and [4h](*p*-TolSO₃) were isolated in 79–99% yields. [4g](*p*-TolSO₃) and [4j](*p*-TolSO₃) decompose for ca. 5 min at room temperature (RT) in solutions as the

solids and they were not isolated from the homogeneous reaction mixtures. However, $[4g]^+$ and $[4i,j]^+$ were detected by HRESI⁺-MS (found, 178.0980 $[4g]^+$; calcd, 178.0975; found, 130.0974 $[4i]^+$; calcd, 130.0975; found, 192.1149 $[4j]^+$; calcd, 192.1131).

Stability of $[4a-j]^+$ can be interpreted in terms of electronic effects of substituents R in the molecules. Thus, if R is a group with strong +M effect, viz. NAlk₂, the cyanide derived part of molecules $[4a-d]^+$ forms guanidinium-like fragment $[R_2N-C(OR)=NH_2]^+$, which exhibits drastic stability due to positive charge delocalization and it is responsible for stability of the salts at RT. Cations $[4e-j]^+$ contain less donor R moieties and degrades in solution within 1–5 h at RT.

It is reported that *metal-bound* O-iminoacylated oximes are quite stable,^{12a,14b,19a,c,21a,22b} whereas the *uncomplexed* species $R'R''C=NOC(=NH)R$ are rather reactive and, right after their preparation, these compounds typically split to the parent amidoximes $R'R''C=NOH$ and nitriles RCN (Scheme 5, a).^{12a,19a,c-e} In the case of good leaving group R'', especially NH₂, heterocyclization to 1,2,4-oxadiazole is observed as a side reaction (b).^{12a}

Scheme 5. Transformations of Iminoacylated Oximes



Stability of iminoacylated oximes strongly depends on R and it is increasing with more electron-withdrawing character of R.^{12a,29} In particular, when R is perfluorinated alkyl, the imines are stable at RT and decompose only upon heating.²⁹ On the contrary, if R is NAlk₂, the imines rapidly and unselectively degrade at RT with half-life ca. 7 min, whereas when R is Et or Ph, having an average electron donor ability, the imines survive for ca. 7 days at RT.^{12a}

Thus, in $[4a-j]^+$, the protonation blocks the electron pair of the highly reactive imine group and it prevents these species from further transformations. Protonation of imines for inhibiting their reactivity is widely used in organic chemistry,^{12a,30} but the protonation has never been applied for stabilization of O-iminoacylated oximes.

Generation of 1,2,4-Oxadiazoles. Dialkylcyanamide derivatives $[4a-d](p\text{-TolSO}_3)$ are stable both in solutions (undried MeOH, Me₂SO) and in the solid state at RT, whereas benzoylcyanamide and aryl and alkyl cyanide derivatives $[4e-j](p\text{-TolSO}_3)$ in these solutions undergo spontaneous conversion at RT for 5 h ($[4e,f](p\text{-TolSO}_3)$), 1 h ($[4h](p\text{-TolSO}_3)$), or less than 5 min ($[4g](p\text{-TolSO}_3)$ and $[4i,j](p\text{-TolSO}_3)$) producing 1,2,4-oxadiazoles **5e–j** and ureas **6a,b** and **6e–g** (Scheme 6). The conversion of $[4](p\text{-TolSO}_3)$ was monitored by ¹H NMR and HRESI-MS until the complete disappearance of the starting salts. ¹H NMR yields of 1,2,4-

oxadiazoles **5a–h** and **5j** (Scheme 6, A) are given in Table S1 (Supporting Information).

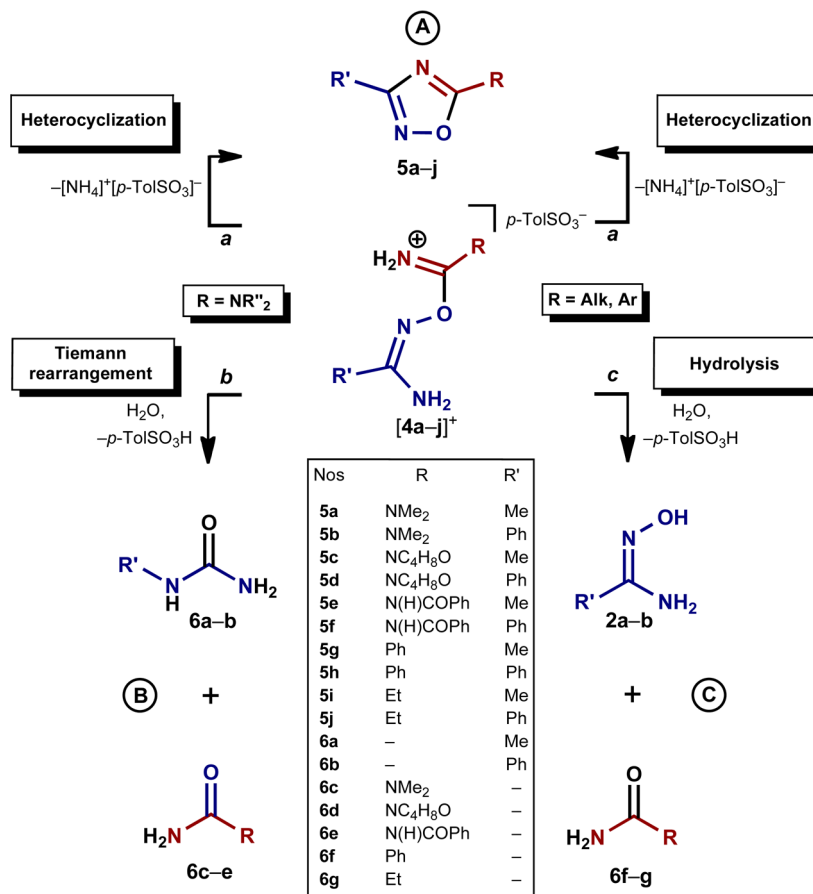
Salts $[4a-f](p\text{-TolSO}_3)$ and $[4h](p\text{-TolSO}_3)$ were dissolved in (CD₃)₂SO, CD₃OD, or a CD₃OD/D₂O mixture (1/1, v/v) at RT and then they were kept at 65 °C for a certain time indicated in Table S1 (Supporting Information). $[4g](p\text{-TolSO}_3)$ and $[4j](p\text{-TolSO}_3)$ were generated *in situ* from **3g** and **3j**, respectively, at 65 °C in the appropriate solvents.

In solutions in the temperature range from 20 to 80 °C, $[4a-f](p\text{-TolSO}_3)$ undergo spontaneous transformations by two routes, i.e., by heterocyclization to achieve 1,2,4-oxadiazoles **5a–f** (Scheme 6, a) and Tiemann rearrangement furnishing substituted ureas **6a–e** (b) (Scheme 6, B). Under the same conditions $[4g-j](p\text{-TolSO}_3)$ undergo the heterocyclization to **5g–j** and hydrolysis to carboxamides **6f,g** and parent amidoximes **2a,b** (c) (Scheme 6, C). Products derived from the hydrolysis of ureas **6c–e**, viz. HNMe₂, OC₄H₈NH, and PhCONH₂ were also observed. In the case of *conventional* nitrile derivatives, starting amidoximes **2a,b** were identified in the reaction mixtures (C). Metal-free organic species **5a,b**, **5d**, **5f–j**, and **6a–g** (A–C) were identified by comparison of their ¹H NMR spectra with the reported spectra (for **5a,b**, **5d**, **5f–j**, see refs 12b and 31; for **6a–e**, see ref 32) or with the spectra of commercially available compounds (for **6f–g**; Aldrich) and, in addition, these species were also identified by GC–MS. Previously unknown heterocycles **5c** and **5e** were isolated from reaction mixtures and characterized by elemental analyses (C, H, N), HRESI-MS, IR, and ¹H and ¹³C{¹H} NMR (Experimental Section).

Noticeably, temperature does not significantly affect the yields of the final compounds. Thus, decreasing the reaction temperature in CD₃OD results in increasing the yield of corresponding **5a–f** (for $[4a-f](p\text{-TolSO}_3)$) for 3–4% per each 10 °C, whereas no obvious temperature dependence was found for $[4g,h](p\text{-TolSO}_3)$ and $[4j](p\text{-TolSO}_3)$. Similar results were observed for the reaction of $[4b](p\text{-TolSO}_3)$ in (CD₃)₂SO. Thus, the yield of **5b** is 69% when the reaction proceeds at 50 °C and completes for 10 days, whereas the yield is 58% when the reaction is conducted at 80 °C for 12 h. Because of a significant drop of the rate of the conversions, we consider 65 °C as the optimal temperature for generation of **5a–h** and **5j**. At this temperature the reaction completes for a rather short time period and gives good yields of the products.

Inspection of the obtained data indicates the drastic dependence of yields and the reaction time for oxadiazoles **5a–j** and ureas **6a–e** and carboxamides **6f,g** on solvent employed. Thus, the preferable solvent for preparation of 3-alkyl-5-amino-1,2,4-oxadiazoles is dimethyl sulfoxide and it is methanol for 3-aryl-5-amino-1,2,4-oxadiazoles. The reactions proceed with similar rates in (CD₃)₂SO and CD₃OD for all cyanamide derived salts $[4a-f](p\text{-TolSO}_3)$, but the heterocyclization is substantially accelerated in CD₃OD/D₂O. Yields of heterocycles **5a–j** were similar when the reaction was performed in commercial wet and absolute CD₃OD.

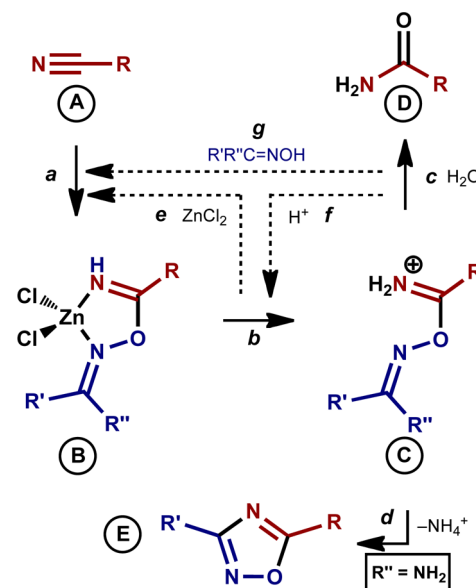
Routes, reaction times, and selectivity of the conversions of $[4a-j](p\text{-TolSO}_3)$ also significantly depend on the nature of substituent R. Thus, the *conventional* nitrile derivatives are much more reactive and completely transform to the oxadiazoles even at RT for 5 h ($[4h](p\text{-TolSO}_3)$) or for 5 min ($[4g](p\text{-TolSO}_3)$ and $[4i-j](p\text{-TolSO}_3)$). Irrespective of the nature of R', yields of the oxadiazoles are the highest in (CD₃)₂SO.

Scheme 6. Conversion of [4a–j](*p*-TolSO₃) to 1,2,4-Oxadiazoles 5a–j, Ureas 6a–g, and Parent Amidoximes 2a,b

The heterocyclization is more efficient for the iminium salts rather than for the corresponding free bases, and [4g–j](*p*-TolSO₃) transform to the oxadiazoles more rapidly and in higher yields than the appropriate unprotonated species. Thus, [4g–j](*p*-TolSO₃) give the heterocycles in ca. 80–90% NMR yields in (CD₃)₂SO for 1 h at RT, whereas the corresponding free iminoacylamidoximes slowly (half-life ca. 5–8 d at RT) transform to the oxadiazoles under the same conditions in 10–30% NMR yields.^{12a}

Differences in the side reactions between [4a–f](*p*-TolSO₃) and [4g–j](*p*-TolSO₃), viz. Tiemann rearrangement and hydrolysis, respectively, can be rationalized by electron donor properties of the substituents. It is known that acid hydrolysis of the guanidine moiety proceeds under harsh conditions due to high stability of the guanidinium cation,³³ whereas the hydrolysis of relevant amidines occurs more smoothly.³⁴ Occurrence of the hydrolysis in the case of [4g–j](*p*-TolSO₃) and its absence for [4a–f](*p*-TolSO₃) is in agreement with the differences in the stability between the guanidinium and the amidinium cations.^{33,34}

Overall Mechanism for the Zn^{II}/H⁺-Assisted Reaction Leading to 1,2,4-Oxadiazoles. We succeeded in isolation and identification of all intermediates of the reaction. On the basis of the experimental data, one can suggest a plausible mechanism of the reported Zn^{II}/H⁺-assisted conversion of nitriles to 1,2,4-oxadiazoles (Scheme 7). The first step of the reaction is formation of zinc complex B by the reaction of nitrile RCN and amidoxime R'C(NH₂)=NOH in the presence of ZnCl₂ (Scheme 7, a). On this step, the zinc(II) center activates nitrile species toward nucleophilic addition and the

Scheme 7. Plausible Mechanism of Zn^{II}/H⁺-Assisted Generation of 1,2,4-Oxadiazoles

reactivity follow the expected pattern R'₂NCN ≥ ArCN > AlkCN.^{17b,18} Most probably reaction proceeds as intramolecular nucleophilic addition between coordinated oxime and activated nitrile ligand, producing five-membered metallacycle. In addition, the metal stabilizes the generated imino species, which are unstable in metal-free state.^{12a}

The second step is protonation of the ligand in B, accompanied by decoordination, and leading to iminium salt C (Scheme 7, *b*). The third step includes intramolecular nucleophilic attack producing heterocycle E from C (Scheme 7, *d*). The metal center does not play any role in the transformations of C to E. Indeed, no effect of ZnCl₂ additions (from 5 to 100 mol % relatively to C) to iminium salts C (any of [4a–f](*p*-TolSO₃) and [4h](*p*-TolSO₃)) on steps *c* and *d* was observed.

It is worth noticing that in the case of aryl and alkyl cyanides, the side reaction of iminoacylated amidoxime is hydrolysis (Scheme 6, *c*) that regenerates the starting amidoxime, which can react with an additional amount of the starting nitrile substrate. Thus, the yield of heterocycle E (Scheme 7) for aryl and alkyl cyanides increases when excess nitrile (80 °C, 48 h) is employed. In the case of the cyanamides R²₂NCN, the side reaction leads to substituted ureas via Tiemann rearrangement (Scheme 6, *b*) and does not regenerate the starting amidoxime and yield of heterocycle E (Scheme 7) only depends on solvent employed (see above).

Thus, 1 equiv of *p*-TolSO₃H·H₂O was added to solutions of 3b, 3h, and 3j in (CD₃)₂SO and the solutions were heated for 48 h (3b) or for 15 min (3h and 3j) to give the corresponding 1,2,4-oxadiazoles (5b, 5h, and 5j) in 64, 78, and 87% NMR yields, respectively. Then 1 equiv of the corresponding nitrile was added to all solutions. Additional heating of the mixtures for 48 h (3b, 3h, and 3j) leads to the quantitative NMR yield of 5h and 5j (respectively to the starting complexes 3h and 3j, correspondingly), whereas the yield of cyanamide derivative 5b was not changed.

Analytical and Spectroscopy Data. Complexes 3a–f and salts [4a–f](*p*-TolSO₃) give satisfactory C, H, and N elemental analyses for the proposed formulas, and these species were also characterized by ATR-FTIR, IR, high resolution ESI-MS, CP-MAS TOSS ¹³C NMR spectroscopy, and single-crystal X-ray diffraction for seven species (3a–e, [4b](*p*-TolSO₃), and [4d](*p*-TolSO₃)). In addition, [4a–f](*p*-TolSO₃) were characterized by ¹H NMR spectroscopy.

The ATR-FTIR spectra of 3a–f and [4a–f](*p*-TolSO₃) display three to five bands from medium to medium-to-strong intensities at 3471–3139 cm⁻¹, which can be attributed to the N–H stretches.³⁵ The IR spectra of all these compounds exhibit two C=N absorption bands in the range 1693–1628 cm⁻¹, which are specific to ligated imines and oximes^{12a,17,19f} (3a–f) and uncomplexed amidinium salts [4a–f](*p*-TolSO₃).³⁵ The spectra of 3e, 3f, [4e](*p*-TolSO₃), and [4f](*p*-TolSO₃) also feature a very strong band in the region 1717–1709 cm⁻¹, characteristic for the C=O stretches of the carboxamide group.³⁵

The positive mode high resolution ESI mass-spectra of complexes 3a–f exhibit several groups of peaks corresponding to the fragmentation ions [L + H]⁺, [M – 2Cl – H]⁺, [M – Cl]⁺, [M – 2Cl – H + L]⁺, [M – Cl + L]⁺, and [M + L + H]⁺, whereas in the negative mode the only observed set of peaks corresponds to [ZnCl₃]⁻. The positive and negative mode ESI spectra of amidinium salts [4a–f](*p*-TolSO₃) display group of peaks from the cation [L + H]⁺ and from the anion [*p*-TolSO₃]⁻, respectively.

The ¹H NMR spectra of [4a–d](*p*-TolSO₃) were recorded in (CD₃)₂SO. The spectra of [4a–d](*p*-TolSO₃) (Figures S11–S14, Supporting Information) featuring two broad singlets in low-field region from the protonated imine group =NH₂⁺, whereas the spectra of [4e](*p*-TolSO₃) and [4f](*p*-TolSO₃)

(Figures S15–S16, Supporting Information) represent only one broad singlet related to this moiety. In addition, the spectra of acetamide derivatives [4a](*p*-TolSO₃) and [4c](*p*-TolSO₃) display two broad singlets from the amide group hydrogens, whereas for other compounds, viz. [4b](*p*-TolSO₃) and [4d–f](*p*-TolSO₃), only one broad signal was observed. Differences in spectra might be related to different structure (and/or dynamics) of the compounds in solution. The spectra of benzoylcyanamide derivatives [4e](*p*-TolSO₃) and [4f](*p*-TolSO₃) do not display both signals from the amide PhC(=O)NH proton and resonance of residual water, which may be a consequence of fast exchange of these hydrogens with H's of water in the solutions in NMR time scale. The spectra of [4a–f](*p*-TolSO₃) exhibit two low-field doublets and one high-field singlet from *p*-TolSO₃⁻.

The solid state CP-MAS TOSS ¹³C NMR spectra of 3a–f (Figures S5–S10, Supporting Information) and [4a–f](*p*-TolSO₃) (Figures S17–S22, Supporting Information), measured due to insufficient solubilities of these species in the most common deuterated solvents, display two signals in the region 168.80–155.02 ppm corresponding to the quaternary C atoms from the carbamidine and the carbamidoxime groups and a set of signals from 146.22 to 125.24 ppm of the C atoms of the aromatic systems (3b, 3d–f, and [4a–f](*p*-TolSO₃)). The spectra of 3e, 3f, [4e](*p*-TolSO₃), and [4f](*p*-TolSO₃) also exhibit a signal in the interval 170.32–168.28 ppm, which can be attributed to C=O. The spectra of 3a–d and [4a–d](*p*-TolSO₃) display two signals of the configurationally non-equivalent C atoms of the dialkylamide group. The spectrum of [4e](*p*-TolSO₃) displays two pairs of signals of the C=O and CH₃–C C atoms, and their appearance could be rationalized by different location of molecules in the lattice or by the presence of different configurations of the molecules in the powdered sample.

X-ray Structure Determinations. Inspection of the structural data indicate that in molecular structures of 3a–e (Figures 1 and 2 and Figures S1–3, Supporting Information) coordination polyhedra of all zinc(II) complexes studied in this work exhibit a typical tetrahedral geometry. All bond angles around the zinc(II) centers range from 103.54(5) to 135.60(16)°, except the N(1)–Zn(1)–N(2) angles, which range from 76.50(18) to 79.15(13)°. The Zn–Cl distances [2.2066(13)–2.2713(6) Å] are specific for the Zn^{II}–Cl bonds.³⁶ The Zn–N(1) bond lengths [1.966(4)–1.995(5) Å] exhibit values characteristic for (imine)Zn^{II} bonds,³⁶ whereas the Zn–N(2) distances [2.0470(17)–2.145(5) Å] are usual for (oxime)Zn^{II} complexes.³⁶

Molecular structures of [4b](*p*-TolSO₃) and [4d](*p*-TolSO₃) (Figures 3 and S4, Supporting Information) represent two types of species in the crystal lattice, viz. amidinium cation and *p*-toluenesulfonate anion. All bond lengths and angles in the anion are typical for *p*-TolSO₃⁻.³⁷

In the molecular structures of 3a–e, [4b](*p*-TolSO₃), and [4d](*p*-TolSO₃), the O(1)–C(1), N(4)–C(2), and N(3)–C(1) (for 3a–d, [4b](*p*-TolSO₃), and [4d](*p*-TolSO₃)) bonds [1.333(2)–1.381(12) Å, 1.315(5)–1.343(2) Å, and 1.325(3)–1.344(6) Å, respectively] are normal single bonds.³⁸ The O(1)–N(2) distances [1.436(12)–1.478(2) Å] are longer than usual O–N^{sp2} bonds,³⁸ and this is specific for *O*-imidoylamidoximes.^{12a,17b} The N(1)–C(1) (3a–d, [4b](*p*-TolSO₃), and [4d](*p*-TolSO₃)) and N(2)–C(2) (3a–e, [4b](*p*-TolSO₃), and [4d](*p*-TolSO₃)) bond lengths [1.281(6)–1.340(16) and 1.295(5)–1.314(7) Å, correspondingly] indicate intermediate

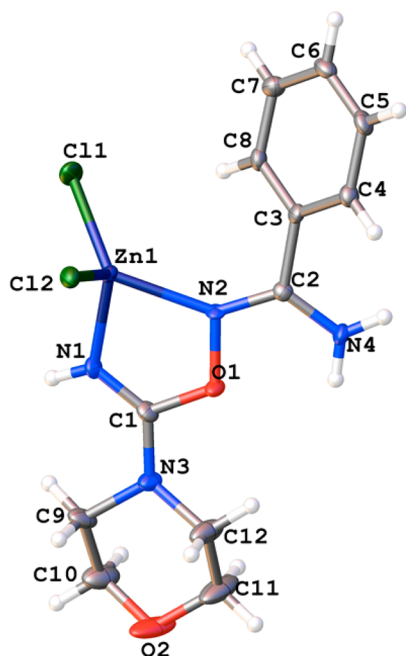


Figure 1. Molecular structure of **3d** with the atomic numbering scheme. Thermal ellipsoids are given at the 50% probability level.

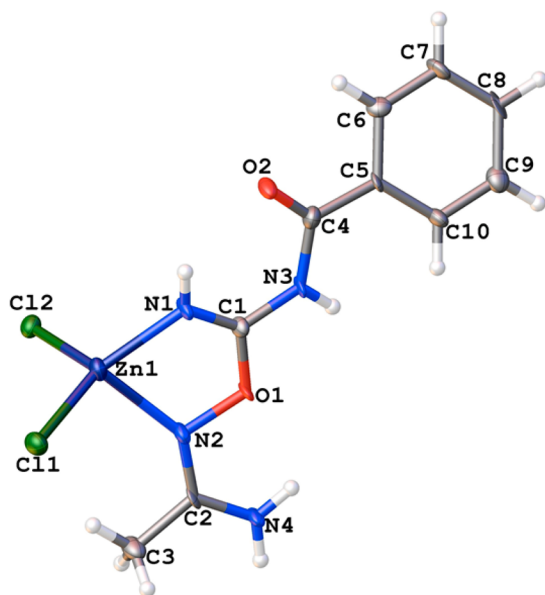


Figure 2. Molecular structure of **3e** with the atomic numbering scheme. Thermal ellipsoids are given at the 50% probability level.

order between single and double bonds, which reflects the amide character of these bonds.³⁸ In the molecular structure of [**4e**](*p*-TolSO₃), the N(1)–C(1) [1.267(7) Å] and O(2)–C(4) [1.226(7) Å] bonds are the conventional double bond,³⁸ whereas the N(3)–C(1) and the N(3)–C(4) bonds [1.388(7) and 1.370(7) Å, respectively] are normal single bonds.³⁸

In **3a–e**, [**4b**](*p*-TolSO₃), and [**4d**](*p*-TolSO₃), *O*-carbamidinediamidoxime adopts the *E*-configuration around the oxime C=N bond and intramolecular hydrogen bond exists between one of the H atoms of the amide group and the O atom of the oxime moiety [N(4)⋯O(1) 2.520–2.560 Å; N(4)–H⋯O(1) 101.38–102.51°], whereas the imine C=N bond in **3a–e** exists in the *Z*-configuration and no intramolecular H-bondings

were detected. Another intramolecular H-bond that was detected in **3e** between the H atom of the amidine group and the O atom of the amide moiety [N(1)⋯O(2) 2.741 Å; N(1)–H⋯O(2) 119.06°] and in [**4b**](*p*-TolSO₃), and [**4d**](*p*-TolSO₃) between one of the H atoms of the amidinium moiety and the oxime N atom [N(1)⋯N(2) 2.522–2.579 Å; N(1)–H⋯N(2) 104.59–107.89°].

FINAL REMARKS

We succeeded in isolation and identification of all intermediates of the Zn^{II}/H⁺-assisted generation of 1,2,4-oxadiazoles and studied their further transformations. First, we observed the Zn^{II}-mediated coupling between RCN's (both cyanamides and conventional nitriles) and amidoximes that gives chelates [ZnCl₂{HN=C(R)ON=C(R')NH₂}] (**3**); this selective integration at the zinc(II) center was not previously reported. Second, in the presence of the strong acid *p*-TolSO₃H, complexes [ZnCl₂{HN=C(R)ON=C(R')NH₂}] (**3**) rapidly liberate the chelated ligand giving the iminium salts [H₂N=C(R)ON=C(R')NH₂](*p*-TolSO₃) ([**4**](*p*-TolSO₃)). The protonation has never been applied for stabilization of reactive *O*-iminoacylated oximes and the suggested procedure provides an easy route to these species. Third, the iminium salts [H₂N=C(R)ON=C(R')NH₂](*p*-TolSO₃) ([**4**](*p*-TolSO₃)) transform to the 1,2,4-oxadiazoles (**5**) in the range from 20 to 65 °C and the heterocyclization is not affected by the presence of the metal. Fourth, cyanamide derivatives [H₂N=C(NR₂)ON=C(R')NH₂](*p*-TolSO₃) ([**4a–f**](*p*-TolSO₃)) are involved in Tiemann rearrangement as a side reaction, whereas aryl and alkyl cyanide derivatives [H₂N=C(R)ON=C(R')NH₂](*p*-TolSO₃) (R = Ar, Alk) ([**4g–j**](*p*-TolSO₃)) undergo partial hydrolysis.

Noticeably, neither generation of nitrile oxides^{12b} (Scheme 2, *d*) was observed under the reaction conditions nor was the formation of 7-membered chelate^{12c} (*a*) detected. Hence, the inorganic chemistry approach allowed for an understanding of the mechanism and driving forces for the Zn^{II}/H⁺-assisted formation of 1,2,4-oxadiazoles. After evaluation of the mechanism of the conversion, we succeeded to increase the yields of the heterocyclization in the cases of aryl and alkyl cyanides to essentially quantitative by performing the syntheses in appropriate solvents and by utilization of excess nitrile. As can be inferred from the inspection of the mechanism depicted in Scheme 7, the generation of the oxadiazoles could be conducted as Zn^{II}-catalyzed rather than Zn^{II}-mediated reaction insofar as the zinc center is involved only in the first step of the transformation, whereupon it is liberated and is ready for the further coupling; preliminary synthetic experiments support this assumption. Works on the catalytic approach to Zn^{II}/H⁺-involved synthesis of 1,2,4-oxadiazoles, as well as application of other metal centers to this reaction, are underway in our group.

EXPERIMENTAL SECTION

Materials and Instrumentation. Solvents were obtained from commercial sources and used as received. The amidoximes³⁹ and benzoyl cyanamide⁴⁰ were synthesized according to the literature methods. Melting points were measured on a Stuart SMP30 apparatus in capillaries and are not corrected. Microanalyses were carried out on a Euro EA3028-HT analyzer. Electrospray ionization mass spectra were obtained on a Bruker micrOTOF spectrometer equipped with an electrospray ionization (ESI) source. The instrument was operated both in positive and in negative ion modes using a *m/z* range 50–3000. The capillary voltage of the ion source was set at –4500 V (ESI⁺-MS) and the capillary exit at ±70–150 V. The nebulizer gas

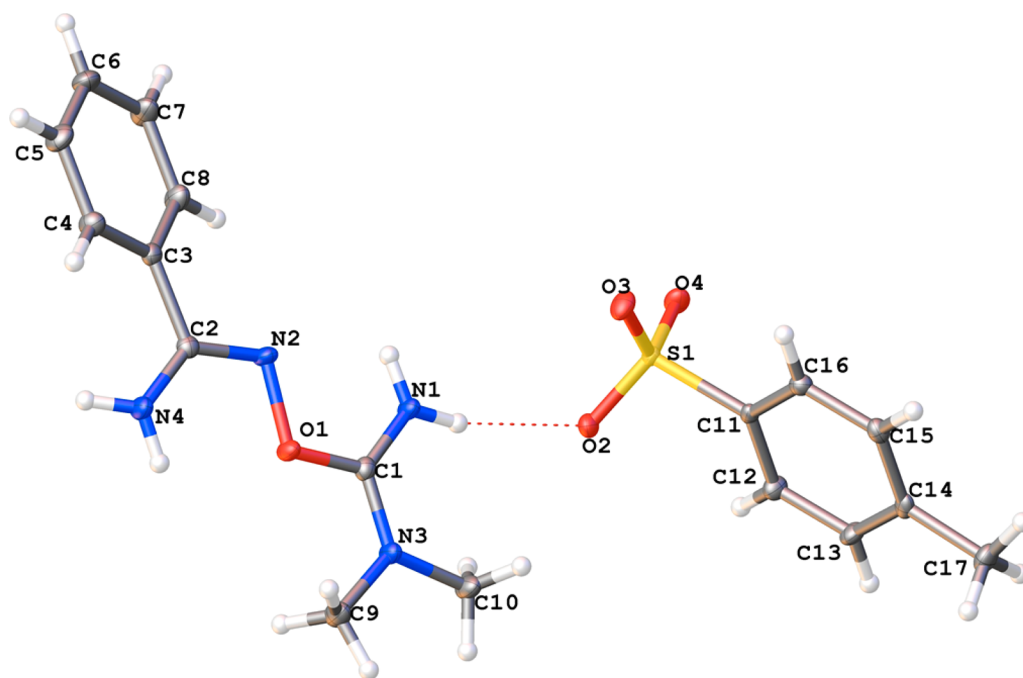


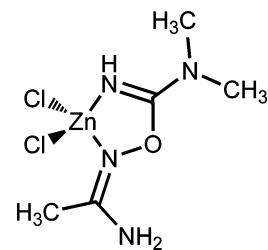
Figure 3. Molecular structure of **4b** with the atomic numbering scheme. Thermal ellipsoids are given at the 50% probability level.

flow was 0.4 bar and the drying gas flow 4.0 L/min. For ESI, species were dissolved in MeOH. In the isotopic pattern, the most intense peak is reported. GC–MS identification of the heterocycles and the urea derivatives was recorded on a Shimadzu GCMS-QP2010 Ultra instrument equipped with Stabilwax 30 m \times 0.32 \times 0.50 μ m column. Temperature program was 70–230 $^{\circ}$ C with a linear rate 10 $^{\circ}$ C/min and holding the column at 230 $^{\circ}$ C for 75 min. ATR-FTIR spectra were obtained on Nicolet 6700 equipped with an ATR-FTIR accessory and Ge/KBr beam splitter. Infrared spectra (4000–400 cm^{-1}) were recorded on a Shimadzu IRPrestige-21 instrument in KBr pellets. ^1H NMR spectra were measured on a Bruker Avance 400 spectrometer in $\text{Me}_2\text{SO}-d_6$ at ambient temperature; residual solvents signals were used as the internal standard. The solid state CP-MAS TOSS ^{13}C NMR spectra were measured on Bruker Avance III WB 400 with magic angle spinning at 6 and 9 kHz frequencies.

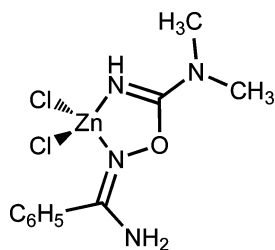
X-ray Structure Determinations. For single crystal X-ray diffraction experiment, crystals of all compounds were fixed on a micro mount and placed on a Agilent Technologies Excalibur Eos diffractometer (**3a–d**, [**4b**](*p*-TolSO₃), [**4d**](*p*-TolSO₃) (high values of the refinement parameters and rather low bonds precision in the structural model are due to the small size and low quality of the crystals)) and were measured using monochromated Mo $K\alpha$ radiation. A crystal of **3e** was placed on a Agilent Technologies SuperNova diffractometer and measured using monochromated Cu $K\alpha$ radiation. All crystals were studied at 100 K. The structures have been solved by the direct methods and refined by means of the SHELXL-97 program⁴¹ incorporated in the OLEX2 program package.⁴² The crystallographic data and some parameters of refinement are placed in Table S2 (Supporting Information). The carbon and nitrogen-bound H atoms were placed in calculated positions and were included in the refinement in the “riding” model approximation, with $U_{\text{iso}}(\text{H})$ set to $1.5U_{\text{eq}}(\text{C})$ and C–H 0.96 Å for the CH₃ groups, $U_{\text{iso}}(\text{H})$ set to $1.2U_{\text{eq}}(\text{C})$ and C–H 0.97 Å for the CH₂ groups, and $U_{\text{iso}}(\text{H})$ set to $1.2U_{\text{eq}}(\text{N})$ and N–H 0.86 Å for the NH₂ and NH groups. Empirical absorption correction was applied in CrysAlisPro program complex⁴³ using spherical harmonics, implemented in SCALE3 ABSPACK scaling algorithm. Supplementary crystallographic data for this paper have been deposited at Cambridge Crystallographic Data Centre and can be obtained free of charge via www.ccdc.cam.ac.uk/data_request/cif.

■ SYNTHETIC WORK

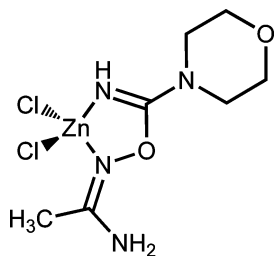
Preparation of 3a–j. Powder of $\text{RC}(=\text{NOH})\text{NH}_2$ ($\text{R} = \text{Me}, \text{Ph}$) (550 μmol ; 40.7 mg or 74.8 mg, respectively) was added to a stirred solution of ZnCl_2 (550 μmol ; 75 mg) in ethyl acetate (5 mL) (**3a–h**) or in propanenitrile (7.5 mL) (**3i–j**) placed in a 10 mL round bottomed flask. After that, the corresponding cyanamide $\text{NCNR}'\text{R}''$ ($\text{R}' = \text{R}'' = \text{Me}$; $\text{R}'\text{R}'' = \text{NC}_4\text{H}_8\text{O}$; $\text{R}' = \text{H}, \text{R}'' = \text{C}(=\text{O})\text{Ph}$) (660 μmol ; 53.5 μL , 66.5 μL , 96.4 mg, respectively; for **3a–f**) or benzonitrile (2.75 mmol; 283.3 μL ($\text{R} = \text{Me}$), 1.10 mmol; 113.3 μL ($\text{R} = \text{Ph}$); for **3g** and **3h**) was added to the mixture. The mixture was kept in a closed flask at 80 $^{\circ}$ C under stirring in air (1000 rpm). After 20 h (**3a–f**) or 48 h (**3g–j**), the mixture was cooled to RT and the solvent was evaporated *in vacuo* at 50 $^{\circ}$ C. Precipitate formed was washed by three 1.5 mL portions of CH_2Cl_2 and dried in air at 50 $^{\circ}$ C for 1 h and after that at RT in air (**3a–h** and **3j**). Complex **3i** is unstable under the reaction conditions and it was characterized by ESI⁺-MS: 227.9876 ($[\text{ZnCl}\{\text{HN}=\text{C}(\text{Et})\text{ON}=\text{C}(\text{Me})\text{NH}_2\}]^+$, calcd 227.9877).



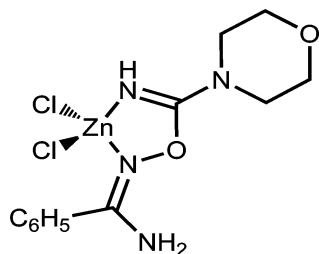
3a. Yield: 89% (137.2 mg). Mp: 175 $^{\circ}$ C (dec). Anal. Calcd for $\text{C}_5\text{H}_{12}\text{N}_4\text{Cl}_2\text{OZn}$: C, 21.41; H, 4.31; N, 19.98. Found: C, 21.67; H, 4.20; N, 19.88. High resolution ESI⁺-MS (MeOH, m/z): 145.1095 ($[\text{L} + \text{H}]^+$, calcd 145.1084), 242.9991 ($[\text{M} - \text{Cl}]^+$, calcd 242.9986), 387.0996 ($[\text{M} - \text{Cl} + \text{L}]^+$, calcd 387.0997), 425.0733 ($[\text{M} + \text{L} + \text{H}]^+$, calcd 425.0734). ATR-FTIR (ZnSe, selected bands, cm^{-1}): 3427 (m), 3343 (m-s) $\nu(\text{N}-\text{H})_{\text{amide}}$, 3312 (m) $\nu(\text{N}-\text{H})_{\text{imine}}$. IR (KBr, selected bands, cm^{-1}): 2937 (w) $\nu(\text{C}-\text{H})$; 1672 (m) $\nu(\text{C}=\text{N})_{\text{oxime}}$; 1630 (s) $\nu(\text{C}=\text{N})_{\text{imine}}$ and $\delta(\text{N}-\text{H})$. CP-MAS TOSS ^{13}C NMR (δ): 161.81, 156.53 ($\text{CH}_3-\text{C}(=\text{N})-\text{NH}_2$ and $\text{O}-\text{C}(=\text{N})-\text{N}(\text{CH}_3)_2$); 40.54, 39.44 ($\text{N}(\text{CH}_3)_2$); 16.33 (CH_3-C). Crystals suitable for X-ray diffraction were obtained by a slow evaporation of a methanol–nitromethane solution at RT in air.



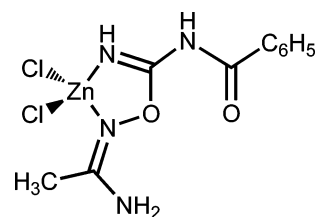
3b. Yield: 96% (180.7 mg). Mp: 157 °C (dec). Anal. Calcd for $C_{10}H_{14}N_4Cl_2O_2Zn$: C, 35.06; H, 4.12; N, 16.36. Found: C, 35.31; H, 4.11; N, 16.62. High resolution ESI⁺-MS (MeOH, m/z): 207.1242 ([L + H]⁺, calcd 207.1240), 305.0140 ([M - Cl]⁺, calcd 305.0142), 511.1311 ([M - Cl + L]⁺, calcd 511.1310), 549.1051 ([M + L + H]⁺, calcd 549.1048). ATR-FTIR (ZnSe, selected bands, cm^{-1}): 3390 (m), 3335 (m-s) $\nu(N-H)_{amide}$; 3321 (sh) $\nu(N-H)_{imine}$. IR (KBr, selected bands, cm^{-1}): 2962 (w), 2932 (w) $\nu(C-H)$; 1659 (s) $\nu(C=N)_{oxime}$; 1643 (vs) $\nu(C=N)_{imine}$ and $\delta(N-H)$. CP-MAS TOSS ¹³C NMR (δ): 162.14, 160.60 ($C_6H_5-C(=N)-NH_2$ and $O-C(=N)-N(CH_3)_2$); 136.24, 131.18, 129.42 (C_6H_5); 40.28, 37.27 ($N(CH_3)_2$). Crystals suitable for X-ray diffraction were obtained by a slow evaporation of methanol–nitromethane solution at RT in air.



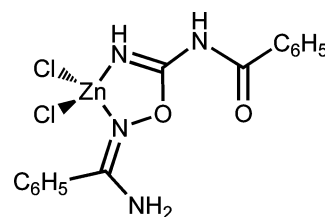
3c. Yield: 86% (178.1 mg). Mp: 151 °C (dec). Anal. Calcd for $C_7H_{14}N_4Cl_2O_2Zn$: C, 26.07; H, 4.38; N, 17.37. Found: C, 26.19; H, 4.52; N, 17.29. High resolution ESI⁺-MS (MeOH, m/z): 187.1198 ([L + H]⁺, calcd 187.1190), 285.0083 ([M - Cl]⁺, calcd 285.0091), 509.0939 ([M + L + H]⁺, calcd 509.0946). ATR-FTIR (ZnSe, selected bands, cm^{-1}): 3419 (m), 3328 (m-s) $\nu(N-H)_{amide}$; 3307 (m) $\nu(N-H)_{imine}$. IR (KBr, selected bands, cm^{-1}): 2955 (w-m), 2920 (w-m), 2860 (w-m) $\nu(C-H)$; 1666 (s) $\nu(C=N)_{oxime}$; 1632 (vs) $\nu(C=N)_{imine}$ and $\delta(N-H)$. CP-MAS TOSS ¹³C NMR (δ): 159.35, 157.10 ($CH_3-C(=N)-NH_2$ and $O-C(=N)-N(CH_2)_2$); 66.38 ($O-(CH_2)_2$); 47.58, 46.72 ($N(CH_2)_2$); 17.13 (CH_3-C). Crystals suitable for X-ray diffraction were obtained by a slow evaporation of methanol–ethyl acetate solution at RT in air.



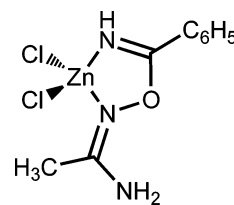
3d. Yield: 87% (183.9 mg). Mp: 142 °C (dec). Anal. Calcd for $C_{12}H_{16}N_4Cl_2O_2Zn$: C, 37.48; H, 4.19; N, 14.57. Found: C, 37.40; H, 4.19; N, 14.66. High resolution ESI⁺-MS (MeOH, m/z): 249.1338 ([L + H]⁺, calcd 249.1346), 347.0243 ([M - Cl]⁺, calcd 347.0248), 595.1516 ([M - Cl + L]⁺, calcd 595.1521), 633.1253 ([M + L + H]⁺, calcd 633.1261). ATR-FTIR (ZnSe, selected bands, cm^{-1}): 3395 (m), 3329 (sh) $\nu(N-H)_{amide}$; 3315 (m) $\nu(N-H)_{imine}$. IR (KBr, selected bands, cm^{-1}): 2968 (w), 2907 (w), 2864 (w) $\nu(C-H)$; 1653 (s) $\nu(C=N)_{oxime}$; 1628 (vs) $\nu(C=N)_{imine}$ and $\delta(N-H)$. CP-MAS TOSS ¹³C NMR (δ): 161.71, 159.13 ($C_6H_5-C(=N)-NH_2$ and $O-C(=N)-N(CH_2)_2$); 133.84, 133.00, 129.57, 128.06, 126.83 (C_6H_5); 67.15 ($O(CH_2)_2$); 45.78 ($N(CH_2)_2$). Crystals suitable for X-ray diffraction were obtained by a slow evaporation of methanol–ethyl acetate solution at RT in air.



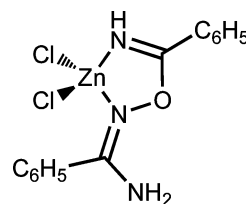
3e. Yield: 95% (190.0 mg). Mp: 193 °C (dec). Anal. Calcd for $C_{10}H_{12}N_4Cl_2O_2Zn$: C, 33.69; H, 3.39; N, 15.72. Found: C, 33.45; H, 3.29; N, 15.98. High resolution ESI⁺-MS (MeOH, m/z): 221.1039 ([L + H]⁺, calcd 221.1033), 283.0181 ([M - 2Cl - H]⁺, calcd 283.0168), 318.9931 ([M - Cl]⁺, calcd 318.9935), 503.1137 ([M - 2Cl - H + L]⁺, calcd 503.1128), 539.0890 ([M - Cl + L]⁺, calcd 539.0895). ATR-FTIR (ZnSe, selected bands, cm^{-1}): 3414 (m), 3338 (m-s), 3243 (m) $\nu(N-H)_{amide}$; 3215 (sh) $\nu(N-H)_{imine}$. IR (KBr, selected bands, cm^{-1}): 3069 (w) $\nu(C-H)$; 1709 (vs) $\nu(C=O)$; 1663 (s) $\nu(C=N)_{oxime}$; 1643 (vs) $\nu(C=N)_{imine}$ and $\delta(N-H)$. CP-MAS TOSS ¹³C NMR (δ): 170.32 (C=O); 159.76, 157.19 ($CH_3-C(=N)-NH_2$ and $O-C(=N)-NH$); 135.84, 134.74, 132.68, 131.73, 129.68, 128.87 (C_6H_5); 16.33 (CH_3). Crystals suitable for X-ray diffraction were obtained by a slow evaporation on methanol–nitromethane solution at RT in air.



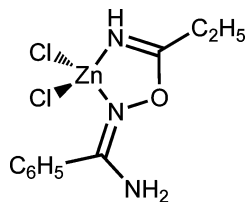
3f. Yield: 93% (211.7 mg). Mp: 113 °C (dec). Anal. Calcd for $C_{15}H_{14}N_4Cl_2O_2Zn$: C, 43.04; H, 3.37; N, 13.38. Found: C, 43.06; H, 3.20; N, 13.68. High resolution ESI⁺-MS (MeOH, m/z): 283.1179 ([L + H]⁺, calcd 283.1190), 381.0080 ([M - Cl]⁺, calcd 381.0091), 627.1404 ([M - 2Cl - H + L]⁺, calcd 627.1441), 663.1197 ([M - Cl + L]⁺, calcd 663.1208). ATR-FTIR (ZnSe, selected bands, cm^{-1}): 3471 (m), 3333 (m-s), 3249 (sh) $\nu(N-H)_{amide}$; 3218 (m-s) $\nu(N-H)_{imine}$. IR (KBr, selected bands, cm^{-1}): 3061 (w), 3005 (w), 2922 (w), 2853 (w) $\nu(C-H)$; 1717 (vs) $\nu(C=O)$; 1659 (m) $\nu(C=N)_{oxime}$; 1636 (vs) $\nu(C=N)_{imine}$ and $\delta(N-H)$. CP-MAS TOSS ¹³C NMR (δ): 168.64 (C=O), 158.54, 155.47 ($C_6H_5-C(=N)-NH_2$ and $O-C(=N)-NH$); 134.20, 131.80, 129.17, 126.65 ($2C_6H_5$).



3g. Yield: 75% (129.3 mg). Mp: 175 °C (dec). Anal. Calcd for $C_{14}H_{13}N_3Cl_2OZn$: C, 34.48; H, 3.54; N, 13.40. Found: C, 34.47; H, 3.61; N, 13.37. High resolution ESI⁺-MS (MeOH, m/z): 178.0986 ([L + H]⁺, calcd 178.0975), 275.9886 ([M - Cl]⁺, calcd 275.9877). ATR-FTIR (ZnSe, selected bands, cm^{-1}): 3403 (m), 3316 (m-s) $\nu(N-H)_{amide}$; 3198 (m-s) $\nu(N-H)_{imine}$. IR (KBr, selected bands, cm^{-1}): 1666 (m) $\nu(C=N)_{oxime}$; 1630 (vs) $\nu(C=N)_{imine}$ and $\delta(N-H)$. CP-MAS TOSS ¹³C NMR (δ): 167.35, 157.72 ($CH_3-C(=N)-NH_2$ and $O-C(=N)-C$); 136.41, 130.61, 129.14, 124.13 (C_6H_5), 17.49 (CH_3).

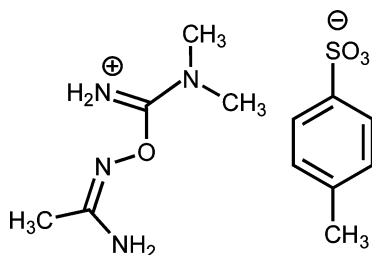


3h. Yield: 87% (179.6 mg). Mp: 189 °C (dec). Anal. Calcd for $C_{14}H_{13}N_3Cl_2OZn$: C, 44.77; H, 3.49; N, 11.19. Found: C, 44.74; H, 3.33; N, 11.36. High resolution ESI⁺-MS (MeOH, m/z): 240.1137 ($[L + H]^+$, calcd 240.1131), 338.0038 ($[M - Cl]^+$, calcd 338.0033). ATR-FTIR (ZnSe, selected bands, cm^{-1}): 3378 (m), 3276 (m-s) $\nu(N-H)_{amide}$, 3181 (m-s) $\nu(N-H)_{imine}$. IR (KBr, selected bands, cm^{-1}): 1630 (m) $\nu(C=N)_{oxime}$ and $\nu(C=N)_{imine}$ and $\delta(N-H)$. CP-MAS TOSS ^{13}C NMR (δ): 166.62, 161.09 ($C_6H_5-C(=N)-NH_2$ and $O-C(=N)-C$); 135.83, 133.03, 130.59, 128.37, 126.19, 123.05 ($2C_6H_5$).

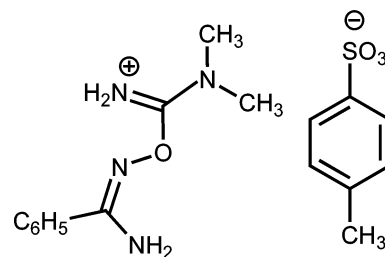


3j. Yield: 88% (158.4 mg). Mp: 134 °C (dec). Anal. Calcd for $C_{14}H_{13}N_3Cl_2OZn$: C, 36.67; H, 4.00; N, 12.83. Found: C, 36.77; H, 4.05; N, 12.80. High resolution ESI⁺-MS (MeOH, m/z): 192.1137 ($[L + H]^+$, calcd 192.1131), 290.0031 ($[M - Cl]^+$, calcd 290.0033). ATR-FTIR (ZnSe, selected bands, cm^{-1}): 3370 (m), 3287 (m-s) $\nu(N-H)_{amide}$, 3189 (m-s) $\nu(N-H)_{imine}$. IR (KBr, selected bands, cm^{-1}): 1631 (m) $\nu(C=N)_{oxime}$ and $\nu(C=N)_{imine}$ and $\delta(N-H)$. ^{13}C NMR (CP-MAS TOSS 9 kHz, δ): CP-MAS TOSS ^{13}C NMR (δ): 176.72, 160.67 ($C_6H_5-C(=N)-NH_2$ and $O-C(=N)-C$); 134.92, 131.64, 130.55, 129.38, 127.01 (C_6H_5); 23.56 (CH_2); 9.68 (CH_3).

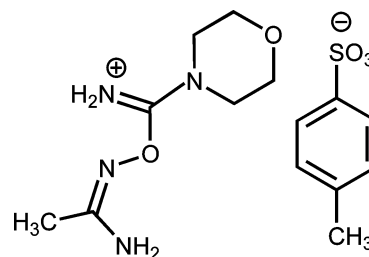
Preparation of [4a–f](*p*-TolSO₃) and [4h](*p*-TolSO₃). Preparation of [4a–d](*p*-TolSO₃) and [4f](*p*-TolSO₃). A solution of *p*-toluenesulfonic acid monohydrate (200 μ mol; 38 mg) in methanol (1 mL) was added to a stirred suspension of any of one 3a–d, 3f, and 3h (190 μ mol) in methanol (1 mL) in a 5 mL round-bottomed flask. After homogenization of the solution (ca. 10 s), the solvent was evaporated *in vacuo* at RT. An oily residue was crystallized under ethyl acetate (1.5 mL) under ultrasound treatment and the precipitate formed was filtered off. Powders of [4a–d](*p*-TolSO₃) were dried at RT in air, whereas powders of [4f](*p*-TolSO₃) and [4h](*p*-TolSO₃) were dried *in vacuo* at 10 mbar for 1 h.



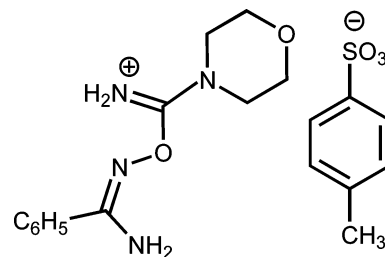
[4a](*p*-TolSO₃). Yield: 97% (58.2 mg). Mp: 123–126 °C (dec). Anal. Calcd for $C_{12}H_{20}N_4O_4S$: C, 45.56; H, 6.37; N, 17.71. Found: C, 45.49; H, 6.45; N, 17.80. High resolution ESI⁺-MS (MeOH, m/z): 145.1087 ($[L + H]^+$, calcd 145.1084). High resolution ESI⁻-MS (MeOH, m/z): 171.0114 ($[p-TolSO_3]^-$, calcd 171.0121). ATR-FTIR (ZnSe, selected bands, cm^{-1}): 3415 (m), 3344 (m) $\nu(N-H)_{amide}$, 3326 (m), 3181 (m-s) $\nu(N-H)_{imine}$. IR (KBr, selected bands, cm^{-1}): 2951 (w), 2922 (w) $\nu(C-H)$; 1693 (vs), 1670 (vs) $\nu(C=N)$; 1165 (vs), 1117 (vs) $\nu(S=O)$. 1H NMR ($(CD_3)_2SO$, δ): 8.66 (s, br, 1H, $=NH_2$), 8.42 (s, br, 1H, $=NH_2$), 7.48 (d, 2H, *o*-CH_{anion}), 7.12 (d, 2H, *m*-CH_{anion}), 7.08 (s, br, 1H, $-NH_2$), 6.81 (s, br, 1H, $-NH_2$), 3.05 (s, br, 6H, $N(CH_3)_2$), 2.29 (s, 3H, CH_3)_{anion}, 1.85 (s, 3H, CH_3). CP-MAS TOSS ^{13}C NMR (δ): 168.80, 159.99 ($CH_3-C(=N)-NH_2$ and $O-C(=N)-N(CH_3)_2$); 144.18, 139.71, 133.22, 129.79, 127.57, 125.24 ($CH_3C_6H_4SO_3$); 37.97 ($N(CH_3)_2$); 20.93 ($CH_3C_6H_4SO_3$); 17.89 (CH_3-C).



[4b](*p*-TolSO₃). Yield: 99% (71.1 mg). Mp: 135–139 °C (dec). Anal. Calcd for $C_{17}H_{22}N_4O_4S$: C, 53.95; H, 5.86; N, 14.80. Found: C, 54.01; H, 5.73; N, 14.87. High resolution ESI⁺-MS (MeOH, m/z): 207.1235 ($[L + H]^+$, calcd 207.1240). High resolution ESI⁻-MS (MeOH, m/z): 171.015 ($[p-TolSO_3]^-$, calcd 171.0121). ATR-FTIR (ZnSe, selected bands, cm^{-1}): 3391 (m), 3336 (m-s) $\nu(N-H)_{amide}$, 3321 (sh), 3215 (w-m) $\nu(N-H)_{imine}$. IR (KBr, selected bands, cm^{-1}): 3065 (w), 2922 (w) $\nu(C-H)$; 1684 (vs), 1647 (vs) $\nu(C=N)$; 1246 (s), 1175 (vs) $\nu(S=O)$. 1H NMR ($(CD_3)_2SO$, δ): 8.76 (s, br, 1H, $=NH_2$), 8.60 (s, br, 1H, $=NH_2$), 7.86 (d, 2H, *o*-CH), 7.58 (t, 1H, *p*-CH), 7.53–7.46 (m, 4H, *o*-CH_{anion} and *m*-CH), 7.35 (s, br, 2H, $-NH_2$), 7.11 (d, 2H, *m*-CH_{anion}), 3.15 (s, br, 3H, NCH_3), 3.11 (s, br, 3H, NCH_3), 2.29 (s, 3H, CH_3)_{anion}. CP-MAS TOSS ^{13}C NMR (δ): 158.87, 156.36 ($C_6H_5-C(=N)-NH_2$ and $O-C(=N)-N(CH_3)_2$); 146.22, 138.75, 133.57, 131.50, 130.99, 130.04, 129.55, 128.04, 126.73 ($C_6H_5 + CH_3C_6H_4SO_3$); 37.84, 36.01 ($N(CH_3)_2$); 21.28 ($CH_3C_6H_4SO_3$). Crystals suitable for X-ray diffraction were obtained by a slow evaporation of acetone solution at RT in air.

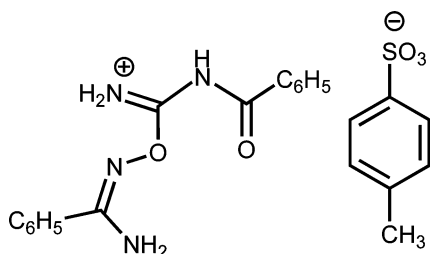


[4c](*p*-TolSO₃). Yield: 98% (66.7 mg). Mp: 91–95 °C (dec). Anal. Calcd for $C_{14}H_{22}N_4O_4S$: C, 46.92; H, 6.19; N, 15.63. Found: C, 46.93; H, 6.39; N, 15.58. High resolution ESI⁺-MS (MeOH, m/z): 187.1201 ($[L + H]^+$, calcd 187.1190). High resolution ESI⁻-MS (MeOH, m/z): 171.0108 ($[p-TolSO_3]^-$, calcd 171.0121). ATR-FTIR (ZnSe, selected bands, cm^{-1}): 3420 (m), 3330 (m-s) $\nu(N-H)_{amide}$, 3310 (sh), 3191 (m) $\nu(N-H)_{imine}$. IR (KBr, selected bands, cm^{-1}): 3188 (w-m), $\nu(C-H)$; 1672 (s), 1642 (s) $\nu(C=N)$; 1186 (s), 1128 (vs) $\nu(S=O)$. 1H NMR ($(CD_3)_2SO$, δ): 8.92 (s, br, 1H, $=NH_2$), 8.65 (s, br, 1H, $=NH_2$), 7.48 (d, 2H, *o*-CH_{anion}), 7.11 (d+s, br, 3H, *m*-CH and $-NH_2$)_{anion}, 6.91 (s, br, 1H, $-NH_2$), 3.73–3.54 (m, 8H, $N(CH_2CH_2)_2O$), 2.29 (s, 3H, CH_3)_{anion}, 1.86 (s, 3H, CH_3). CP-MAS TOSS ^{13}C NMR (δ): 161.77, 159.44 ($CH_3-C(=N)-NH_2$ and $O-C(=N)-N(CH_2)_2$); 142.37, 141.25, 140.39, 139.43, 130.35, 126.26 ($CH_3C_6H_4SO_3$); 68.29, 65.72 ($O(CH_2)_2$); 44.83, 44.35 ($N(CH_2)_2$); 22.80 ($CH_3C_6H_4SO_3$); 19.35 (CH_3-C).

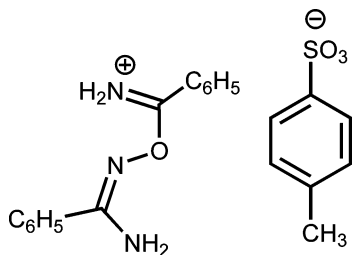


[4d](*p*-TolSO₃). Yield: 93% (74.2 mg). Mp: 123–128 °C (dec). Anal. Calcd for $C_{19}H_{24}N_4O_4S$: C, 54.27; H, 5.75; N, 13.32. Found: C, 54.19; H, 5.62; N, 13.47. High resolution ESI⁺-MS (MeOH, m/z): 249.1348 ($[L + H]^+$, calcd 249.1346). High resolution ESI⁻-MS (MeOH, m/z): 171.0117 ($[p-TolSO_3]^-$, calcd 171.0121). ATR-FTIR (ZnSe, selected bands, cm^{-1}): 3390 (m), 3324 (m) $\nu(N-H)_{amide}$

3279 (m), 3239 (m-s) $\nu(\text{N—H})_{\text{iminium}}$. IR (KBr, selected bands, cm^{-1}): 2986 (w), 2928 (w), 2868 (w) $\nu(\text{C—H})$; 1676 (s), 1659 (vs) $\nu(\text{C=N})$; 1200 (s), 1182 (vs) $\nu(\text{S=O})$. $^1\text{H NMR}$ ($(\text{CD}_3)_2\text{SO}$, δ): 9.07 (s, br, 1H, $=\text{NH}_2$), 8.82 (s, br, 1H, $=\text{NH}_2$), 7.86 (d, 2H, *o*-CH), 7.58 (t, 1H, *p*-CH), 7.53–7.46 (m, 4H, *o*-CH_{anion} and *m*-CH), 7.43 (s, br, 2H, $-\text{NH}_2$), 7.11 (d, 2H, *m*-CH_{anion}), 3.83–3.50 (m, 8H, $\text{N}(\text{CH}_2\text{CH}_2)_2$), 2.29 (s, 3H, CH_3)_{anion}. CP-MAS TOSS $^{13}\text{C NMR}$ (δ): 159.61, 155.02 ($\text{C}_6\text{H}_5\text{—C(=N)—NH}_2$ and $\text{O—C(=N)—N}(\text{CH}_2)_2$); 145.14, 140.79, 131.42, 130.10, 128.72, 127.57, 126.74 ($\text{C}_6\text{H}_5 + \text{CH}_3\text{C}_6\text{H}_4\text{SO}_3$); 65.57, 63.67 ($\text{O}(\text{CH}_2)_2$); 43.93 ($\text{N}(\text{CH}_2)_2$); 21.99 ($\text{CH}_3\text{C}_6\text{H}_4\text{SO}_3$). Crystals suitable for X-ray diffraction were obtained by a slow evaporation of a methanol–nitromethane solution at RT in air.



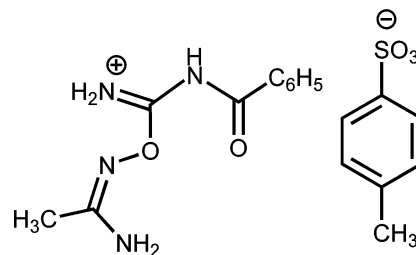
[4f](*p*-TolSO₃). Yield: 79% (68.2 mg). Mp: 138–146 °C (dec). Anal. Calcd for $\text{C}_{22}\text{H}_{22}\text{N}_4\text{O}_5\text{S}$: C, 58.14; H, 4.88; N, 12.33. Found: C, 57.99; H, 4.76; N, 12.49. High resolution ESI⁺-MS (MeOH, m/z): 283.1184 ([L + H]⁺, calcd 283.1190), 565.2293 ([2L + H]⁺, calcd 565.2306), 737.2464 ([2L + H + *p*-TolSO₃H]⁺, calcd 737.2500). High resolution ESI⁻-MS (MeOH, m/z): 171.0163 ([*p*-TolSO₃]⁻, calcd 171.0121). ATR-FTIR (ZnSe, selected bands, cm^{-1}): 3419 (m), 3342 (m-s), 3297 (m-s) $\nu(\text{N—H})_{\text{amide}}$, 3239 (m), 3139 (m) $\nu(\text{N—H})_{\text{iminium}}$. IR (KBr, selected bands, cm^{-1}): 3067 (w), 3024 (w), 2916 (w) $\nu(\text{C—H})$; 1711 (vs) $\nu(\text{C=O})$; 1653 (m), 1647 (s) $\nu(\text{C=N})$; 1177 (s), 1125 (m-s) $\nu(\text{S=O})$. $^1\text{H NMR}$ ($(\text{CD}_3)_2\text{SO}$, δ): 10.32 (s, br, 2H, $=\text{NH}_2$), 8.06 (d, 2H, *o*-CH), 7.92 (d, 2H, *o*-CH), 7.74 (t, 1H, *p*-CH), 7.62 (t, 2H, *m*-CH), 7.60 (t, 1H, *p*-CH), 7.53 (t, 2H, *m*-CH), 7.48 (d, 2H, *o*-CH_{anion}), 7.37 (s, br, 2H, $-\text{NH}_2$), 7.12 (d, 2H, *m*-CH_{anion}), 2.29 (s, 3H, CH_3)_{anion}. CP-MAS TOSS $^{13}\text{C NMR}$ (δ): 168.28 (C=O); 160.40, 155.32 ($\text{C}_6\text{H}_5\text{—C(=N)—NH}_2$ and O—C(=N)—NH); 143.49, 140.83, 133.40, 131.44, 130.35, 128.59 ($2\text{C}_6\text{H}_5$ and $\text{CH}_3\text{C}_6\text{H}_4\text{SO}_3$); 20.25 ($\text{CH}_3\text{C}_6\text{H}_4\text{SO}_3$).



[4h](*p*-TolSO₃). Yield: 88% (68.7 mg). Mp: 118–125 °C (dec). Anal. Calcd for $\text{C}_{21}\text{H}_{21}\text{N}_3\text{O}_4\text{S}$: C, 61.30; H, 5.14; N, 10.21. Found: C, 61.80; H, 5.17; N, 10.17. High resolution ESI⁺-MS (MeOH, m/z): 240.1136 ([L + H]⁺, calcd 240.1131). High resolution ESI⁻-MS (MeOH, m/z): 171.0122 ([*p*-TolSO₃]⁻, calcd 171.0121). ATR-FTIR (ZnSe, selected bands, cm^{-1}): 3315 (m), 3205 (m) $\nu(\text{N—H})_{\text{amide}}$, 3059 (m), 2996 (m-s) $\nu(\text{N—H})_{\text{iminium}}$. IR (KBr, selected bands, cm^{-1}): 2933 (w), 2907 (w) $\nu(\text{C—H})$; 1671 (vs), 1655 (vs) $\nu(\text{C=N})$; 1165 (vs), 1117 (vs) $\nu(\text{S=O})$. $^1\text{H NMR}$ ($(\text{CD}_3)_2\text{SO}$, δ): 10.88 (s, br, 2H, $=\text{NH}_2$), 8.33 (d, 2H, *o*-CH), 7.95 (d, 2H, *o*-CH), 7.86 (t, 1H, *p*-CH), 7.77 (s, br, 2H, $-\text{NH}_2$), 7.69 (t, 2H, *m*-CH), 7.62 (t, 1H, *p*-CH), 7.54 (t, 2H, *m*-CH), 7.50 (d, 2H, *o*-CH_{anion}), 7.12 (d, 2H, *m*-CH_{anion}), 2.29 (s, 3H, CH_3)_{anion}. CP-MAS TOSS $^{13}\text{C NMR}$ (δ): 171.02, 159.6 ($\text{C}_6\text{H}_5\text{—C(=N)—NH}_2$ and $\text{O—C(=N)—C}_6\text{H}_5$); 138.25, 136.05, 132.14, 130.14, 129.74, 129.07, 128.31, 125.97, 124.54 ($2\text{C}_6\text{H}_5$ and $\text{CH}_3\text{C}_6\text{H}_4\text{SO}_3$); 21.23 ($\text{CH}_3\text{C}_6\text{H}_4\text{SO}_3$).

Preparation of [4e](*p*-TolSO₃). A solution of *p*-TolSO₃H·H₂O (190 μmol ; 36.1 mg) in methanol (1 mL) was added to a stirred suspension of **3e** (190 μmol) in methanol (1 mL) placed in a 5 mL round

bottomed flask. After homogenization of the solution (ca. 10 s), solid tetramethylammonium chloride (380 μmol ; 41.6 mg) was added to the solution and the reaction mixture left to stand for 5 min, whereupon the solvent was evaporated *in vacuo* at RT. A precipitate formed was treated with acetone (5 mL), and the solution was separated by filtration from the solid (NMe_4)₂[ZnCl₄]. The solvent was evaporated *in vacuo* at RT, and an oily residue was crystallized from acetone–hexane mixture (0.4 and 2.0 mL, correspondingly). Powder of [4e](*p*-TolSO₃) contaminated with ca. 4 mol % (based upon $^1\text{H NMR}$) (NMe_4)₂[ZnCl₄] was dried at 10 mbar for 1 h at RT.



[4e](*p*-TolSO₃). Yield: 87% (64.8 mg, calcd for pure substance). Mp: 135–145 °C (dec). Anal. Calcd for $\text{C}_{17}\text{H}_{20}\text{N}_4\text{O}_5\text{S}$: C, 52.03; H, 5.14; N, 14.28. Found: C, 52.10; H, 4.98; N, 14.15. High resolution ESI⁺-MS (MeOH, m/z): 221.1042 ([L + H]⁺, calcd 221.1033), 613.2169 ([2L + H + *p*-TolSO₃H]⁺, calcd 613.2187). High resolution ESI⁻-MS (MeOH, m/z): 171.0123 ([*p*-TolSO₃]⁻, calcd 171.0121). ATR-FTIR (ZnSe, selected bands, cm^{-1}): 3425 (m), 3371 (m), 3333 (sh) $\nu(\text{N—H})_{\text{amide}}$, 3317 (m-s), 3212 (m-s) $\nu(\text{N—H})_{\text{iminium}}$. IR (KBr, selected bands, cm^{-1}): 2922 (w), 2854 (w), 2781 (w) $\nu(\text{C—H})$; 1709 (vs) $\nu(\text{C=O})$; 1686 (m), 1647 (vs) $\nu(\text{C=N})$; 1179 (s), 1123 (s) $\nu(\text{S=O})$. $^1\text{H NMR}$ ($(\text{CD}_3)_2\text{SO}$, δ): 10.18 (s, br, 2H, $=\text{NH}_2$), 8.05 (d, 2H, *o*-CH), 7.73 (t, 1H, *p*-CH), 7.59 (t, 2H, *m*-CH), 7.48 (d, 2H, *o*-CH_{anion}), 7.31 (s, br, 1H, $-\text{NH}_2$), 7.12 (d, 2H, *m*-CH_{anion}), 6.78 (s, br, 1H, $-\text{NH}_2$), 2.30 (s, 3H, CH_3)_{anion}, 1.91 (s, 3H, CH_3). CP-MAS TOSS $^{13}\text{C NMR}$ (δ): 170.19, 167.38 (C=O); 161.42, 158.91 ($\text{CH}_3\text{—C(=N)—NH}_2$ and O—C(=N)—NH); 143.45, 142.50, 140.17, 133.22, 132.11, 129.66, 128.21, 126.36 (C_6H_5 and $\text{CH}_3\text{C}_6\text{H}_4\text{SO}_3$); 22.58 ($\text{CH}_3\text{C}_6\text{H}_4\text{SO}_3$); 16.79, 15.83 ($\text{CH}_3\text{—C}$).

Generation of Iminoacyl Amidoximes and Monitoring of Their Further Conversions. A mixture of any of the imino complexes *trans*-PtCl₄[HN=C(R)ON=C(R')NH₂]₂ (R/R' = Et/Me, Et/CH₂Ph, Et/Ph, Ph/Ph) (0.06 mmol) and NaCN (17.7 mg, 0.36 mmol) was dissolved in DMSO-*d*₆ (0.56 mL) at room temperature to produce the uncomplexed imine HN=C(R)ON=C(R')NH₂. The completeness of the liberation was monitored by $^1\text{H NMR}$. The product was detected by $^1\text{H NMR}$ spectroscopy after 5 min, whereupon it was characterized by $^{13}\text{C}\{^1\text{H}\}$ NMR method (total acquisition time is ca. 2 h). ^1H and $^{13}\text{C}\{^1\text{H}\}$ NMR monitoring indicates the iminoacyl amidoximes, after the liberation, undergo further conversion by two routes to give, first, the parent nitrile and amidoxime in the *retro*-coupling and, second, to produce 3,5-substituted 1,2,4-oxadiazoles. Generation of these heterocycles was confirmed by comparison of their NMR characteristics with those for the corresponding oxadiazoles obtained by the independent syntheses.^{12a}

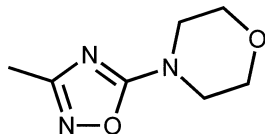
Generation of Previously Known **5a–b**, **5d**, **5f–g**, **5h**, and **5j**.

Salts [4a–b](*p*-TolSO₃), [4d](*p*-TolSO₃), [4f–g](*p*-TolSO₃), [4h](*p*-TolSO₃), and [4j](*p*-TolSO₃) (30 μmol) were dissolved in (CD_3)₂SO, CD_3OD , or a $\text{CD}_3\text{OD}/\text{D}_2\text{O}$ mixture (1/1, v/v) (600 μL) at RT and then they were kept at 65 °C for certain time indicated in Table S1 (Supporting Information). [4g](*p*-TolSO₃) and [4j](*p*-TolSO₃) were generated *in situ* from **3g** and **3j** (30 μmol), respectively, at 65 °C in the appropriate solvents. The completeness of the reaction and yields of the heterocycles were determined by $^1\text{H NMR}$.

Preparation of 3-Methyl-5-(4-morpholyl)-1,2,4-oxadiazole.

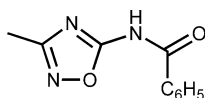
Iminium salt [4c](*p*-TolSO₃) (419 μmol ; 150.0 mg) was dissolved in methanol–water mixture (1.5/1.5 mL) at RT, and the solution was kept at 65 °C for 12 h, whereupon the reaction mixture was treated with water (5 mL) and the title heterocycle was extracted with two 10

mL portions of dichloromethane. The organic phase was dried over anhydrous Na_2SO_4 for 3 h, and the resulting solution was passed through 1 cm^3 of silica gel (Merck 70–230 Mesh). The solvent was evaporated *in vacuo* to give a colorless powder of **5c**.



5c. Yield: 75% (53.1 mg). Mp: 78–80 °C. Anal. Calcd for $\text{C}_7\text{H}_{11}\text{N}_3\text{O}_2$: C, 49.70; H, 6.55; N, 24.84. Found: C, 49.66; H, 6.54; N, 24.77. High resolution ESI⁺-MS (MeOH, *m/z*): 170.0923 ($[\text{M} + \text{H}]^+$, calcd 170.0924), 192.0741 ($[\text{M} + \text{Na}]^+$, calcd 192.0743). IR (KBr, selected bands, cm^{-1}): 2978 (s), 2934 (s), 2874 (s) $\nu(\text{C}-\text{H})$; 1632 (s), 1620 (s) $\nu(\text{C}=\text{N})$. ^1H NMR (CDCl_3 , δ): 2.23 (s, 3H, CH_3), 3.61 (t, 4H, $\text{N}(\text{CH}_2)_2$), 3.78 (t, 4H, $\text{O}(\text{CH}_2)_2$). $^{13}\text{C}\{^1\text{H}\}$ NMR (CDCl_3 , δ): 170.83, 167.86 ($\text{O}-\text{C}(\text{N})-\text{N}(\text{CH}_2)_2$ and $\text{Me}-\text{C}(\text{N})-\text{N}$); 66.04 ($\text{O}(\text{CH}_2)_2$); 45.88 ($\text{N}(\text{CH}_2)_2$); 11.86 (CH_3).

Preparation of 3-Methyl-5-(benzoylamino)-1,2,4-oxadiazole. Complex **3e** (522 μmol ; 190.0 mg) was dissolved in a solution of *p*-TolSO₃H·H₂O (550 μmol ; 104.5 mg) in dimethyl sulfoxide (2.5 mL). The solution obtained was kept at 65 °C for 1 h, whereupon a solution of Na₂S·H₂O (550 μmol ; 132 mg) in H₂O (12 mL) was added and colorless precipitate of ZnS was formed. After 15 min the precipitate was filtered off and the solution was treated by EtOAc (two 10 mL portions). The organic phase was separated and dried over anhydrous Na₂SO₄. The volume of the solution was reduced to ca. 5 mL *in vacuo*, and hexane (15 mL) was added to the solution. Colorless precipitate formed was filtered off and dried at RT in air.



5e. Yield: 71% (75.2 mg). Mp: 145 °C. Anal. Calcd for $\text{C}_{10}\text{H}_9\text{N}_3\text{O}_2$: C, 59.11; H, 4.46; N, 20.68. Found: C, 59.17; H, 4.46; N, 20.88. High resolution ESI⁺-MS (MeOH, *m/z*): 204.0759 ($[\text{M} + \text{H}]^+$, calcd 204.0768), 226.0577 ($[\text{M} + \text{Na}]^+$, calcd 226.0587). High resolution ESI⁻-MS (MeOH, *m/z*): 202.0613 ($[\text{M} - \text{H}]^-$, calcd 202.0611). IR (KBr, selected bands, cm^{-1}): 2928 (w) $\nu(\text{C}-\text{H})$; 1632 (vs) $\nu(\text{C}=\text{O})$; 1572 (s) $\nu(\text{C}=\text{N})_{\text{oxime}}$; 1558 (vs) $\nu(\text{C}=\text{N})_{\text{nitrile}}$ and $\delta(\text{N}-\text{H})$. ^1H NMR ($(\text{CD}_3)_2\text{SO}$, δ): 8.14 (d, br, 2H, *o*-CH), 7.49 (m, 3H, *m*-, *p*-CH), 2.29 (s, 3H, CH_3). $^{13}\text{C}\{^1\text{H}\}$ NMR ($(\text{CD}_3)_2\text{SO}$, δ): 175.21, 170.45 ($\text{O}-\text{C}(\text{N})-\text{N}(\text{CH}_2)_2$ and $\text{Me}-\text{C}(\text{N})-\text{N}$); 167.22 ($\text{C}=\text{O}$); 135.64, 134.45, 129.02, 128.10 (C_6H_5); 16.36 (CH_3).

■ ASSOCIATED CONTENT

Supporting Information

Tables of ^1H NMR yields of 1,2,4-oxadiazoles and crystal data. Molecular structures. ^{13}C and ^1H NMR spectra. CIF file. This material is available free of charge via the Internet at <http://pubs.acs.org>.

■ AUTHOR INFORMATION

Corresponding Authors

*N. A. Bokach. E-mail: n.bokach@spbu.ru.

*V. Yu. Kukushkin. E-mail: kukushkin@vk2100.spb.edu.

Notes

The authors declare no competing financial interest.

■ ACKNOWLEDGMENTS

We thank Russian Science Foundation (grant 14-13-00060) for the support of this study. Physicochemical studies were performed at Center for Magnetic Resonance, Center for X-ray Diffraction Studies, and Center for Chemical Analysis and Materials Research, and “Geomodel” Center (all belong to Saint Petersburg State University). D.S.B. is grateful for Saint

Petersburg State University for Rector’s scholarship for Ph.D. students.

■ REFERENCES

- (1) (a) Pace, A.; Pierro, P. *Org. Biomol. Chem.* **2009**, *7*, 4337–4348. (b) Pace, A.; Buscemi, S.; Vivona, N. *Org. Prep. Proced. Int.* **2005**, *37*, 447–506. (c) Hemming, K. 1,2,4-Oxadiazoles. In *Comprehensive Heterocyclic Chemistry III*; Elsevier: Amsterdam, 2008; Vol. 5, pp 243–314. (d) Kayukova, L. A. *Pharm. Chem. J.* **2005**, *39*, 539–547.
- (2) (a) Bokach, N. A.; Khripun, A. V.; Kukushkin, V. Yu.; Haukka, M.; Pombeiro, A. J. L. *Inorg. Chem.* **2003**, *42*, 896–903. (b) Gallardo, H.; Cristiano, R.; Vieira, A. A.; Neves Filho, R. A. W.; Srivastava, R. M.; Bechtold, I. H. *Liq. Cryst.* **2008**, *35*, 857–863. (c) Silva, R. O.; Neves Filho, R. A. W.; Azevedo, R.; Srivastava, R. M.; Gallardo, H. *Struct. Chem.* **2010**, *21*, 485–494.
- (3) Outirite, M.; Lagrenee, M.; Lebrini, M.; Traisnel, M.; Jama, C.; Vezin, H.; Bentiss, F. *Electrochim. Acta* **2010**, *55*, 1670–1681.
- (4) Burns, A. R.; Kerr, J. H.; Kerr, W. J.; Passmore, J.; Paterson, L. C.; Watson, A. J. B. *Org. Biomol. Chem.* **2010**, *8*, 2777–2783.
- (5) (a) Ispikoudi, M.; Amvrazis, M.; Kontogiorgis, C.; Koumbis, A. E.; Litinas, K. E.; Hadjipavlou-Litina, D.; Fylaktakidou, K. C. *Eur. J. Inorg. Chem.* **2010**, *45*, 5635–5645. (b) Bora, R. O.; Dar, B.; Pradhan, V.; Farooqui, M. *Mini Rev. Med. Chem.* **2014**, *14*, 355–369.
- (6) (a) dos Santos Filho, J. M.; Leite, A. C. L.; Galdino de Oliveira, B.; Moreira, D. R. M.; Lima, M. S.; Soares, M. B. P.; Leite, L. F. C. C. *Bioorg. Med. Chem.* **2009**, *17*, 6682–6691. (b) Rai, N. P.; Narayanaswamy, V. K.; Govender, T.; Manuprasad, B. K.; Shashikanth, S.; Arunachalam, P. N. *Eur. J. Med. Chem.* **2010**, *45*, 2677–2682.
- (7) (a) dos Anjos, J. V.; Neves, R. A. W.; do Nascimento, S. C.; Srivastava, R. M.; de Melo, S. J.; Sinou, D. *Eur. J. Med. Chem.* **2009**, *44*, 3571–3576. (b) Kemnitzner, W.; Kuemmerle, J.; Zhang, H. Z.; Kasibhatla, S.; Tseng, B.; Drewe, J.; Cai Sui, X. *Bioorg. Med. Chem. Lett.* **2009**, *19*, 4410–4415. (c) Khan, I.; Ibrar, A.; Abbas, N. *Arch. Pharm.* **2014**, *347*, 1–20.
- (8) Kiss, L. E.; Ferreira, H. S.; Torrao, L.; Bonifacio, M. J.; Palma, P. N.; Soares-da-Silva, P.; Learmonth, D. A. *J. Med. Chem.* **2010**, *53*, 3396–3411.
- (9) Neves Filho, R. A. W.; Aguiar da Silva, C.; Borges da Silva, C. S.; Brustein, V. P.; Navarro, D. M. A. F.; Brayner dos Santos, F. A.; Alves, L. C.; Cavalcanti, M. G. S.; Srivastava, R. M.; Carneiro-Da-Cunha, M. G. *Chem. Pharm. Bull.* **2009**, *57*, 819–825.
- (10) Hemming, K.; Khan, M. N.; O’Gorman, P. A.; Pitard, A. *Tetrahedron* **2013**, *69*, 1279–1284.
- (11) Su, D.; Duan, H.; Wei, Zh.; Cao, J.; Liang, D.; Lin, Y. *Tetrahedron Lett.* **2013**, *54*, 6959–6963.
- (12) (a) Bolotin, D. S.; Bokach, N. A.; Haukka, M.; Kukushkin, V. Y. *ChemPlusChem.* **2012**, *77*, 31–40. (b) Augustine, J. K.; Akabote, V.; Hegde, S. G.; Alagarsamy, P. *J. Org. Chem.* **2009**, *74*, 5640–5643. (c) Yarovenko, V. N.; Ugrak, B. I.; Krayushkin, M. M.; Shirinyan, V. Z.; Zavarzin, I. V. *Russ. Chem. Bull.* **1994**, *43*, 627–629. (d) Yarovenko, V. N.; Taralashvili, V. K.; Zavarzin, I. V.; Krayushkin, M. M. *Tetrahedron* **1990**, *46*, 3941–3952.
- (13) Yarovenko, V. N.; Zavarzin, I. V.; Krayushkin, M. M. *Bull. Acad. Sci. USSR* **1986**, *35*, 1106–1106.
- (14) (a) Bokach, N. A.; Kukushkin, V. Yu. *Coord. Chem. Rev.* **2013**, *257*, 2293–2316. (b) Bokach, N. A.; Kukushkin, V. Y. *Russ. Chem. Rev.* **2005**, *74*, 153–170. (c) Bokach, N. A.; Kuznetsov, M. L.; Kukushkin, V. Y. *Coord. Chem. Rev.* **2011**, *255*, 2946–2967. (d) Pombeiro, A. J. L.; Kukushkin, V. Yu. *Compr. Coord. Chem. II* **2004**, *1*, 639–660. (e) Pombeiro, A. J. L.; Kukushkin, V. Yu. *Compr. Coord. Chem. II* **2004**, *1*, 585–594. (f) Kukushkin, V. Yu.; Pombeiro, A. J. L. *Chem. Rev.* **2002**, *102*, 1771–1802.
- (15) (a) Ahmed, T. J.; Knapp, S. M. M.; Tyler, D. R. *Coord. Chem. Rev.* **2011**, *255*, 949–974. (b) Hvastijova, M.; Kohout, J.; Buchler, J. W.; Boca, R.; Kozisek, J.; Jager, L. *Coord. Chem. Rev.* **1998**, *175*, 17–42. (c) Kobayashi, M.; Shimizu, S. *Curr. Opin. Chem. Biol.* **2000**, *4*, 95–102. (d) Michelin, R. A.; Sgarbossa, P.; Mazzega Sbovata, S.; Gandin, V.; Marzano, C.; Bertani, R. *ChemMedChem.* **2011**, *6*, 1172–

1183. (e) Murahashi, S.-I.; Takaya, H. *Acc. Chem. Res.* **2000**, *33*, 225–233. (f) Corain, B.; Basato, M.; Veronese, A. C. *J. Mol. Catal. A: Chem.* **1993**, *81*, 133–155. (g) Eglin, J. L. *Comments Inorg. Chem.* **2002**, *23*, 23–43. (h) Parkins, A. W. *Platinum Metals Rev.* **1996**, *40*, 169–174. (i) Michelin, R. A.; Mozzon, M.; Bertani, R. *Coord. Chem. Rev.* **1996**, *147*, 299–338. (j) Chin, J. *Acc. Chem. Res.* **1991**, *24*, 145–152. (k) Neumüller, B. Z. *Anorg. Allg. Chem.* **2007**, *633*, 193–204. (l) Kukushkin, Yu. N. *Russ. J. Coord. Chem.* **1998**, *24*, 173–176.
- (16) (a) Kukushkin, V. Yu.; Tudela, D.; Pombeiro, A. J. L. *Coord. Chem. Rev.* **1996**, *156*, 333–362. (b) Kukushkin, V. Yu.; Pombeiro, A. J. L. *Coord. Chem. Rev.* **1999**, *181*, 147–175.
- (17) (a) Bolotin, D. S.; Bokach, N. A.; Kritchenkov, A. S.; Haukka, M.; Kukushkin, V. Yu. *Inorg. Chem.* **2013**, *52*, 6378–6389. (b) Bolotin, D. S.; Bokach, N. A.; Haukka, M.; Kukushkin, V. Yu. *Inorg. Chem.* **2012**, *51*, 5950–5964.
- (18) (a) Kritchenkov, A. S.; Bokach, N. A.; Haukka, M.; Kukushkin, V. Yu. *Dalton Trans.* **2011**, *40*, 4175–4182. (b) Anisimova, T. B.; Bokach, N. A.; Dolgushin, F. M.; Kukushkin, V. Yu. *Dalton Trans.* **2013**, *42*, 12460–12467.
- (19) (a) Makarycheva-Mikhailova, A. V.; Haukka, M.; Bokach, N. A.; Garnovskii, D. A.; Galanski, M.; Keppler, B. K.; Pombeiro, A. J. L.; Kukushkin, V. Y. *New J. Chem.* **2002**, *26*, 1085–1091. (b) Makarycheva-Mikhailova, A. V.; Bokach, N. A.; Haukka, M.; Kukushkin, V. Yu. *Inorg. Chim. Acta* **2003**, *356*, 382–386. (c) Kukushkin, V. Yu.; Pakhomova, T. B.; Bokach, N. A.; Wagner, G.; Kuznetsov, M. L.; Galanski, M.; Pombeiro, A. J. L. *Inorg. Chem.* **2000**, *39*, 216–225. (d) Kukushkin, V. Yu.; Pakhomova, T. B.; Kukushkin, Yu. N.; Herrmann, R.; Wagner, G.; Pombeiro, A. J. L. *Inorg. Chem.* **1998**, *37*, 6511–6517. (e) Garnovskii, D. A.; Pombeiro, A. J. L.; Haukka, M.; Sobota, P.; Kukushkin, V. Yu. *Dalton Trans.* **2004**, 1097–1103. (f) Garnovskii, D. A.; Guedes da Silva, M. F. C.; Pakhomova, T. B.; Wagner, G.; Duarte, M. T.; Frausto da Silva, J. J. R.; Pombeiro, A. J. L.; Kukushkin, V. Y. *Inorg. Chim. Acta* **2000**, 499–504. (g) Luzyanin, K. V.; Kukushkin, V. Yu.; Kuznetsov, M. L.; Garnovskii, D. A.; Haukka, M.; Pombeiro, A. J. L. *Inorg. Chem.* **2002**, *41*, 2981–2986. (h) Luzyanin, K. V.; Kukushkin, V. Yu.; Haukka, M.; Frausto da Silva, J. J. R.; Pombeiro, A. J. L. *Dalton Trans.* **2004**, 2728–2732. (i) Wagner, G.; Pombeiro, A. J. L.; Kukushkin, Yu. N.; Pakhomova, T. B.; Ryabov, A. D.; Kukushkin, V. Y. *Inorg. Chim. Acta* **1999**, *292*, 272–275.
- (20) (a) Ferreira, C. M. P.; Guedes da Silva, M. F. C.; Frausto da Silva, J. J. R.; Pombeiro, A. J. L.; Kukushkin, V. Yu.; Michelin, R. A. *Inorg. Chem.* **2001**, *40*, 1134–1142. (b) Lasri, J.; Charmier, M. A. J.; Guedes da Silva, M. F. C.; Pombeiro, A. J. L. *Dalton Trans.* **2006**, 5062–5067. (c) Lasri, J.; Guedes da Silva, M. F. C.; Charmier, M. A. J.; Pombeiro, A. J. L. *Eur. J. Inorg. Chem.* **2008**, *23*, 3668–3677.
- (21) (a) Wagner, G.; Pombeiro, A. J. L.; Bokach, N. A.; Kukushkin, V. Y. *Dalton Trans.* **1999**, 4083–4086. (b) Luzyanin, K. V.; Kukushkin, V. Yu.; Haukka, M.; Pombeiro, A. J. L. *Inorg. Chem. Commun.* **2006**, *9*, 732–735.
- (22) (a) Kim, M.; Lee, J.; Lee, H.-Y.; Chang, S. *Adv. Synth. Catal.* **2009**, *351*, 1807–1812. (b) Kukushkin, V. Yu.; Ilichev, I. V.; Wagner, G.; Frausto da Silva, J. J. R.; Pombeiro, A. J. L. *Dalton Trans.* **1999**, 3047–3052. (c) Kukushkin, V. Yu.; Ilichev, I. V.; Zhdanova, M. A.; Wagner, G.; Pombeiro, A. J. L. *Dalton Trans.* **2000**, 1567–1572.
- (23) (a) Grigg, J.; Collison, D.; Garner, C. D.; Helliwell, M.; Tasker, P. A.; Thorpe, J. M. *J. Chem. Soc., Chem. Commun.* **1993**, 1807–1809. (b) Zerbib, V.; Robert, F.; Gouzerh, P. *J. Chem. Soc., Chem. Commun.* **1994**, 2179–2180.
- (24) Garnovskii, D. A.; Bokach, N. A.; Pombeiro, A. J. L.; Haukka, M.; Frausto da Silva, J. J. R.; Kukushkin, V. Yu. *Eur. J. Inorg. Chem.* **2005**, *2005*, 3467–3471.
- (25) (a) Kopylovich, M. N.; Kirillov, A. M.; Tronova, E. A.; Haukka, M.; Kukushkin, V. Yu.; Pombeiro, A. J. L. *Eur. J. Inorg. Chem.* **2010**, 2425–2432. (b) Kopylovich, M. N.; Haukka, M.; Kirillov, A. M.; Kukushkin, V. Yu.; Pombeiro, A. J. L. *Inorg. Chem. Commun.* **2008**, *11*, 117–120. (c) Pavlishchuk, V. V.; Kolotilov, S. V.; Addison, A. W.; Prushan, M. J.; Butcher, R. J.; Thompson, L. K. *Inorg. Chem.* **1999**, *38*, 1759–1766. (d) Pavlishchuk, V. V.; Kolotilov, S. V.; Addison, A. W.; Prushan, M. J.; Butcher, R. J.; Thompson, L. K. *Chem. Commun.* **2002**, 468–469. (e) Kopylovich, M. N.; Haukka, M.; Kirillov, A. M.; Kukushkin, V. Yu.; Pombeiro, A. J. L. *Chem.–Eur. J.* **2007**, *13*, 786–791. (f) Kopylovich, M. N.; Pombeiro, A. J. L.; Fischer, A.; Kloos, L.; Kukushkin, V. Yu. *Inorg. Chem.* **2003**, *42*, 7239–7248.
- (26) Kopylovich, M. N.; Kukushkin, V. Yu.; Guedes da Silva, M. F. C.; Haukka, M.; Frausto da Silva, J. J. R.; Pombeiro, A. J. L. *J. Chem. Soc., Perkin Trans.* **2001**, 1569–1573.
- (27) Kopylovich, M. N.; Kukushkin, V. Yu.; Haukka, M.; Frausto da Silva, J. J. R.; Pombeiro, A. J. L. *Inorg. Chem.* **2002**, *41*, 4798–4804.
- (28) Morosin, B.; Lingafelter, E. C. *Acta Crystallogr.* **1959**, *12*, 611–612.
- (29) Kabakchi, E. V.; Il'in, V. V.; Ignatenko, A. V.; Ponomarenko, V. A. *Izv. Akad. Nauk, Ser. Khim.* **1993**, *8*, 1453–1458.
- (30) (a) Sellmann, D.; Thallmair, E. *J. Organomet. Chem.* **1979**, *164*, 337–352. (b) Vicente, J.; Chicote, M.-T.; Guerrero, R.; Vicente-Hernandez, I.; Jones, P. G. *Inorg. Chem.* **2003**, *42*, 7644–7651. (c) Bokach, N. A.; Kukushkin, V. Y.; Haukka, M.; Frausto da Silva, J. J. R.; Pombeiro, A. J. L. *Inorg. Chem.* **2003**, *42*, 3602–3608.
- (31) (a) Hammam, A. E. F. G.; Gattas, A. A.; Youssif, N. M. *Egypt. J. Chem.* **1985**, *27*, 515–523. (b) Eloy, F.; Lenaers, R. *Helv. Chim. Acta* **1966**, *49*, 1430–1432. (c) Chennakrishnareddy, G.; Debasis, H.; Jayan, R.; Manjunatha, S. G. *Tetrahedron Lett.* **2011**, *52*, 6170–6173. (d) Barrans, J. *Compt. Rend.* **1959**, *249*, 1096–1098. (e) Perez, M. A.; Dorado, C. A.; Soto, J. L. *Synthesis* **1983**, 483–486. (f) Buscemi, S.; Cicero, M. G.; Vivona, N.; Caronna, T. *J. Heterocycl. Chem.* **1988**, *25*, 931–935. (g) Young, T. E.; Beidler, W. T. *J. Org. Chem.* **1985**, *50*, 1182–1186.
- (32) (a) Artuso, E.; Degani, I.; Fochi, R.; Magistris, C. *Synthesis* **2007**, 3497–3506. (b) Hacker, H.-G.; Meusel, M.; Aschfalk, M.; Gutschow, M. *ACS Comb. Sci.* **2011**, *13*, 59–64. (c) Lorenz, J. C.; Busacca, C. A.; Feng, X.; Grinberg, N.; Haddad, N.; Johnson, J.; Kapadia, S.; Lee, H.; Saha, A.; Sarvestani, M.; Spinelli, E. M.; Varsolona, R.; Wei, X.; Zeng, X.; Senanayake, C. H. *J. Org. Chem.* **2010**, *75*, 1155–1161. (d) Hosgen, R.; Grashey, R.; Krischke, R. *Justus Liebig's Ann. Chem.* **1977**, *3*, 506–527. (e) Bittner, S.; Assaf, Y.; Krief, P.; Pomerantz, M.; Ziemnicka, B. T.; Smith, C. G. *J. Org. Chem.* **1985**, *50*, 1712–1718.
- (33) Limatibul, S.; Watson, J. W. *J. Org. Chem.* **1971**, *36*, 3805–3807.
- (34) Ono, M.; Tamura, S. *Chem. Pharm. Bull.* **1990**, *38*, 590–596.
- (35) Bellamy, L. J. *The infra-red spectra of complex molecules*; Methuen and Co. Ltd.: London, John Wiley and sons, Inc.: New York, 1958.
- (36) Orpen, A. G.; Brammer, L.; Allen, F. H.; Kennard, O.; Watson, D. G.; Taylor, R. *J. Chem. Soc., Dalton Trans.* **1989**, *12*, S1–S83.
- (37) (a) Bincy, I. P.; Gopalakrishnan, R. *Acta Crystallogr., Sect. E* **2013**, *E69*, o1277–o1277. (b) Muralidharan, S.; Nagapandiselvi, P.; Srinivasan, T.; Gopalakrishnan, R.; Velmurugan, D. *Acta Crystallogr., Sect. E* **2013**, *E69*, o804–o804. (c) Kavitha, C. N.; Butcher, R. J.; Jasinski, J. P.; Yathirajan, H. S.; Dayananda, A. S. *Acta Crystallogr., Sect. E* **2013**, *E69*, o485–o486.
- (38) Allen, F. H.; Kennard, O.; Watson, D. G.; Brammer, L.; Orpen, A. G.; Taylor, R. *J. Chem. Soc., Perkin Trans.* **1987**, *12*, S1–S19.
- (39) (a) La, M. C.; Sartini, S.; Salerno, S.; Simorini, F.; Taliani, S.; Marini, A. M.; Da, S. F.; Marinelli, L.; Limongelli, V.; Novellino, E. *J. Med. Chem.* **2008**, *51*, 3182–3193. (b) Bakunov, S. A.; Rukavishnikov, A. V.; Tkachev, A. V. *Synthesis* **2000**, *8*, 1148–1159.
- (40) Nagasawa, H. T.; Kwon, Ch.-H. Acylated cyanamide composition for increasing blood acetaldehyde as an alcoholism deterrent. 1987, WO8704348 A1 19870730.
- (41) Sheldrick, G. M. *Acta Crystallogr., Sect. A* **2008**, *A64*, 112–122.
- (42) Dolomanov, O. V.; Bourhis, L. J.; Gildea, R. J.; Howard, J. A. K.; Puschmann, H. *J. Appl. Crystallogr.* **2009**, *42*, 339–341.
- (43) *CrysAlisPro*, 1.171.36.20; Agilent Technologies: Santa Clara, CA, 27-06-2012.